Effects of Madagascar Mountain Range on Tropical Cyclone Tracks. Part I: Classification of Cyclone Tracks Reaching the East Coast

ZO A. P. H. RAKOTOMAVO
Meteorology Department, University of Antananarivo, Madagascar
Present position: Trainee Engineer at the Madagascar National Meteorological Office

NIRIVOLOLONA RAHOLIJAO
Applied Research Service, Madagascar National Meteorological Office

YUH-LANG LIN
Department of Physics, and Department of Energy & Environmental Systems, and NOAA ISET Center, North Carolina A&T State University, Greensboro, North Carolina

March 30th, 2011

Contents

List of Figures

List of Tables

1. Introduction

This study is performed in order to initiate the investigation of the orographic effects induced by Madagascar mountain range on westward moving tropical cyclone (TC) tracks. Several studies were carried out for typhoons passing over Taiwan's Central Mountain Range (e.g., Brand and Blelloch 1974; Yeh and Elsberry 1993a; Lin et al. 1999, 2002, 2005, 2006, 2011; also see reviews in Lin 2007), and track deflection of tropical cyclones by its central mountain range has been thoroughly studied. Orographic influences on tropical cyclone passage have also been studied over the Hispaniola Mountains in the Caribbean Sea, and the mountains on Luzon in Philippines (Bender et al. 1987). In order to improve the prediction of TC tracks and intensity, a similar study is then started for TCs passing over Madagascar's mountain range which has an average height of 1200 m, with massifs above 2600 m (Fig. 1).

The aim of this initial study is to examine the track deflection of tropical cyclones when they approach and cross over Madagascar's mountain range. In order to do so, a climate study is then introduced here through a classification of cyclone tracks making landfall over the east coast of the island. This classification will also allow us to find if there is a discontinuity of the cyclone track for each track type.

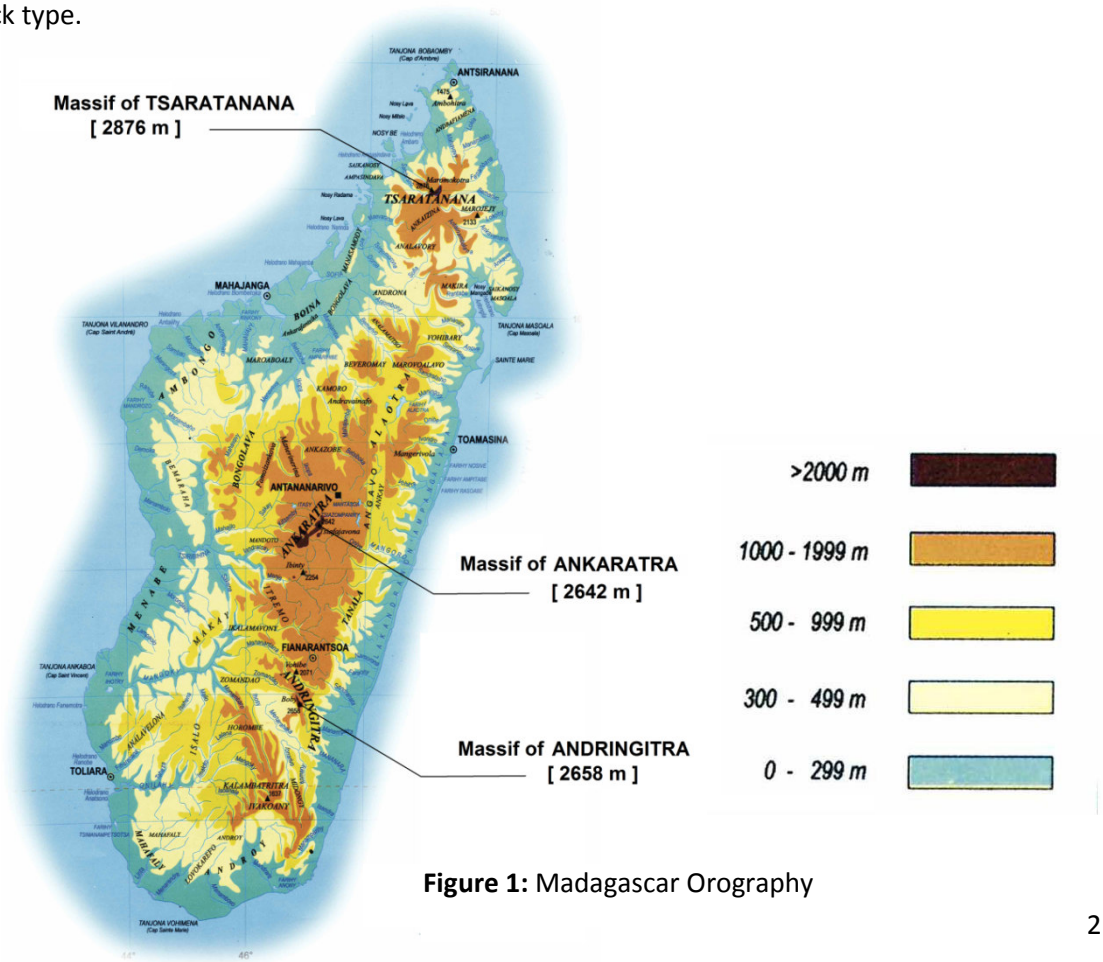

Figure 1: Madagascar Orography

2. Data and Methodology

In this study, we classified the 68 cyclone tracks reaching the east coast of Madagascar during the period 1963 - 2010 (48 cyclonic seasons). A manual classification is conducted based on the analysis of the best-track of the Regional Specialized Meteorological Center (RSMC) of Reunion, available from the Applied Research Service of the Madagascar National Meteorological Office.

Since this study is performed in order to study the orographic effects on tropical cyclones making landfall over the east coast of Madagascar, we classified the cyclone tracks into eight categories according to the following criteria:

- The latitude of the landfall location, and
- The way the tropical cyclone center passed the island.

3. Results and Discussion

3.1. Classification of Cyclone Tracks

According to the above classification criteria, the following five types of cyclone tracks reaching the east coast of Madagascar can be identified:

- **Type A:** landfall location to the north of the latitude 17°S
  - **Type A1:** landfalling to the north of 14°S and entering into the Mozambique Channel to the north of 17°S (Fig. 2);
  - **Type A2:** landfalling between 14°S and 17°S and entering into the Mozambique Channel to the north of 17°S (Fig. 3);
  - **Type A3:** landfalling to the north of 17°S and entering into the Mozambique Channel to the south of 17°S (Fig. 4).

- **Type B:** landfall location between the latitudes 17°S and 20°S
  - **Type B1:** passing almost straight over Madagascar and Mozambique Channel, and then landfalling on Mozambique (Fig. 5);
  - **Type B2:** entering into the Mozambique Channel anticyclonically to the south of 20°S (Fig. 6).

- **Type C:** landfalling to the south of 20°S (Fig. 7*)*
- **Type D:** landfalling on eastern Madagascar and then curving anticyclonically back to the Indian Ocean (Fig. 8)
- **Type E:** looping or erratic cyclone tracks over the Indian Ocean and eastern Madagascar (Fig. 9)

3.1.1 Type A Track

The tropical cyclones landfalling to the north of the latitude 17°S are categorized as Type A cyclones. Under this category, there are three subcategories to be described in the following.

(1) Type A1

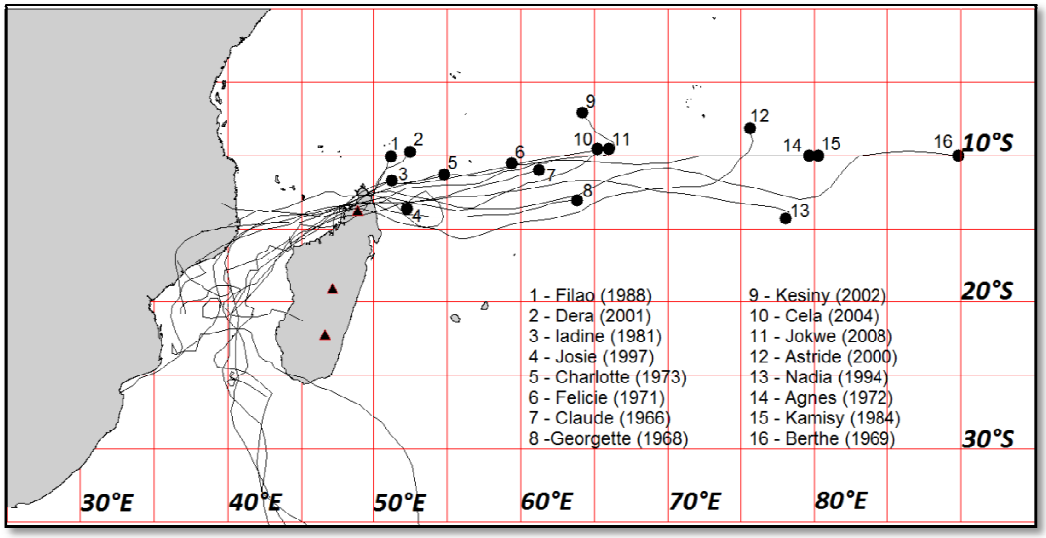

Figure 2: Type A1 track – Landfalling to the north of 14°S and curving into the Mozambique Channel to the north of 17°S.

Type A1 is generally associated with tropical cyclones that move westward before crossing Madagascar to the north of the latitude 14°S and curve southward into the Mozambique Channel. We should note that these cyclone tracks are deflected slightly to the north before they encounter the massif of Tsaratanana (peak coordinates: 49.0°E / 14.0°S).

(2) Type A2

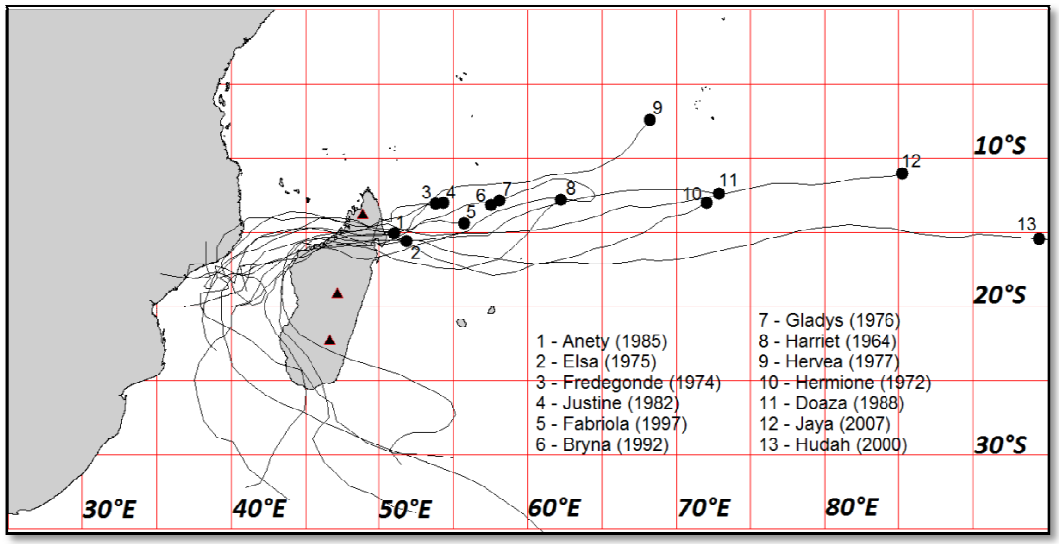

Figure 3: Type A2 track – Landfalling between 14°S – 17°S and curving into the Mozambique Channel to the north of 17°S.

Type A2 cyclones also move westward, like those of Type A1, but reach the east coast of Madagascar between the latitudes 14°S and 17°S. These cyclone tracks are deflected to the south as they encounter the massif of Tsaratanana. After crossing the island, they then curve into the Mozambique Channel anticyclonically at a location to the north of the latitude 17°S. After curving, some of the cyclones landfall on the southwest coast of Madagascar. The track curving in this area is mainly controlled by synoptic systems, in particular the westerly moving troughs and the High over southern Indian Ocean, and has nothing to do with the mountains in Madagascar. The cyclone landfalling on the southwest coast of Madagascar after curving from Mozambique, however, may be influenced by the mountains in the south.

(3) Type A3

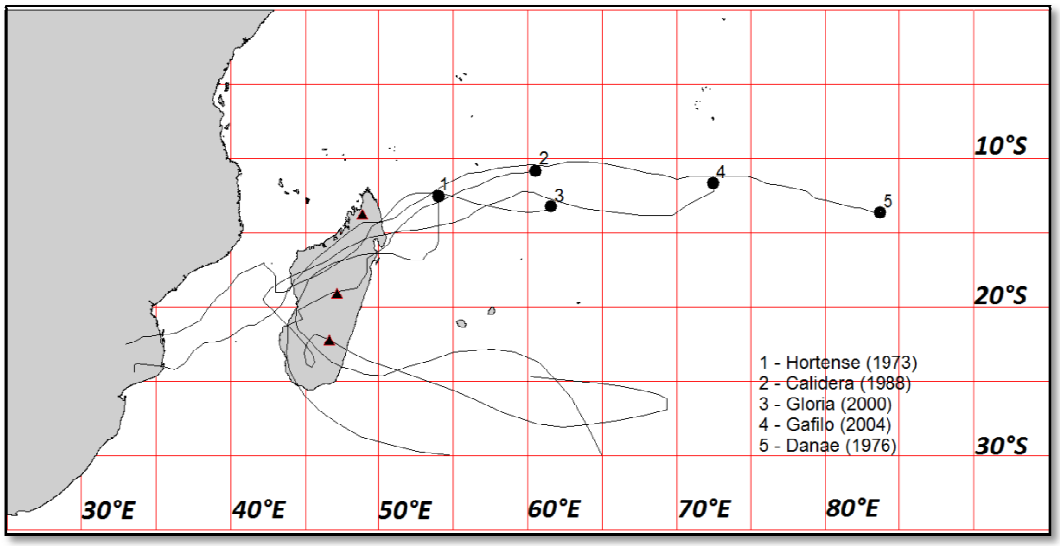

Figure 4: Type A3 track – Landfalling to the north of 17°S and entering into the Mozambique Channel to the south of 17°S.

Type A3 cyclones landfall to the north of 17°S and move toward southwest as they cross Madagascar. Therefore, they reach the east coast of Madagascar to the north of the latitude 17°S and enter into the Mozambique Channel to the south of the latitude 17°S.The majority of this type of cyclones pass through the gap between the Massif of Tsaratanana and the Massif of Ankaratra from northeast to southwest, thus it appears that their tracks are less affected by mountains. However, we can observe some southward deflections near the massif of Tsaratanana's peak (49.0°E / 14.0°S), and some northward deflections near the massif of Ankaratra's peak (47.2°E / 19.3°S). In addition, those cyclones curving back to or making second landfall on the southwest coast of the island may be influenced by the Massif of Andringitra or Ivakoany Massif.

3.1.2 Type B Track

The tropical cyclones landfalling between 17°S and 20°S are categorizes as Type B cyclones. Under this category, there are two subcategories to be described in the following.

(1) Type B1

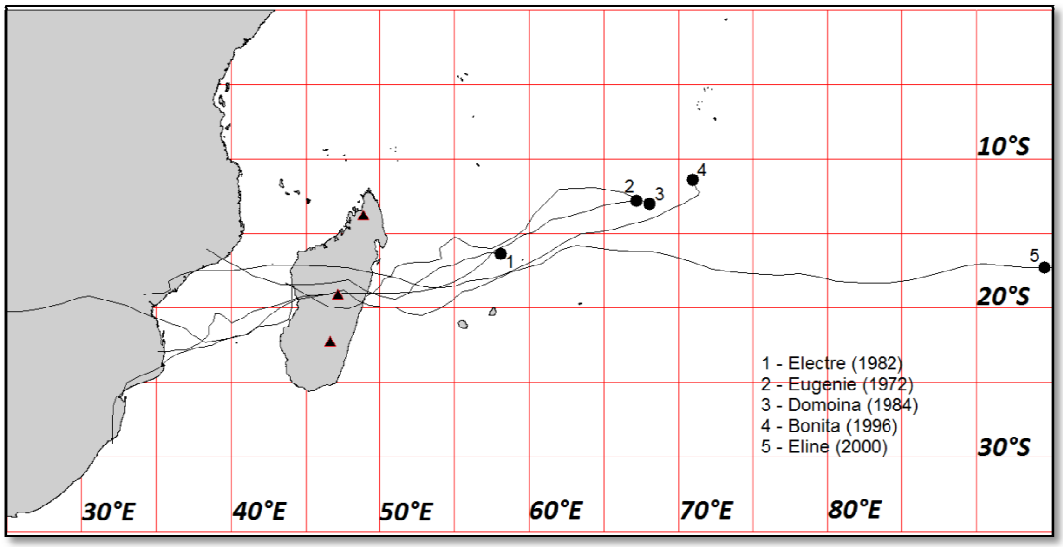

Figure 5: Type B1 track – Landfalling between 17°S and 20°S and entering into the Mozambique Channel to the north of 20°S.

Type B1 cyclones move straight westward before crossing Madagascar between the latitudes 17°S and 20°S, and do not curve after crossing the island. Therefore, they also enter into the Mozambique Channel between 17°S and 20°S. In addition, we must note some northward and southward deflections as the cyclone tracks encounter the massif of Ankaratra (peak coordinates: 47.2°E / 19.3°S).

(2) Type B2

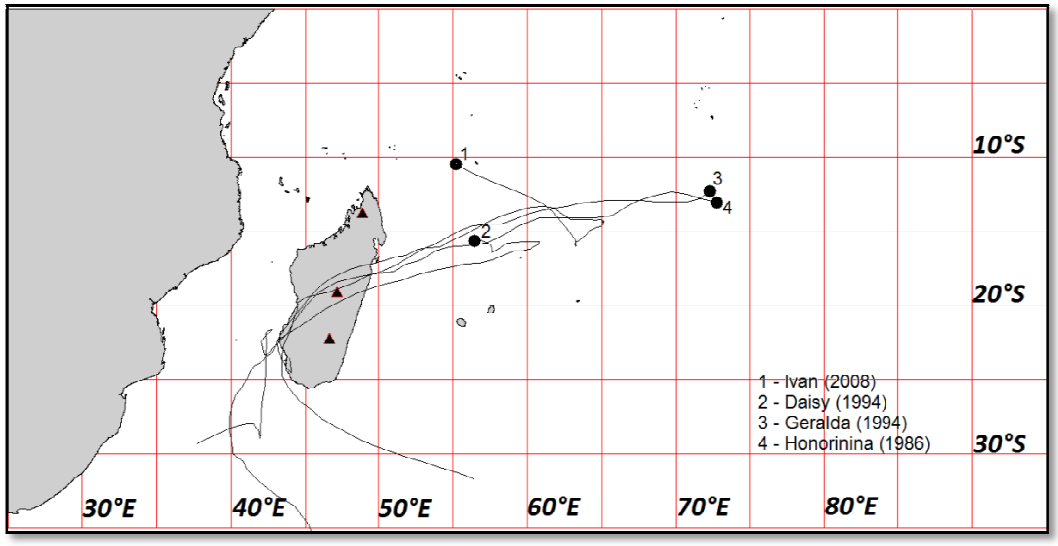

Figure 6: Type B2 track – Landfalling between 17°S and 20°S and curving into the Mozambique Channel to the south of 20°S.

Cyclones belonging to this category (Type B2) landfall in between 17°S and 20°S, move toward the southwest as they cross Madagascar, and enter into the Mozambique Channel to the south of 20°S. Track deflections in this category are not obvious even if they generally pass to the north of the massif of Ankaratra's peak (47.2°E / 19.3°S).

3.1.3 Type C Track

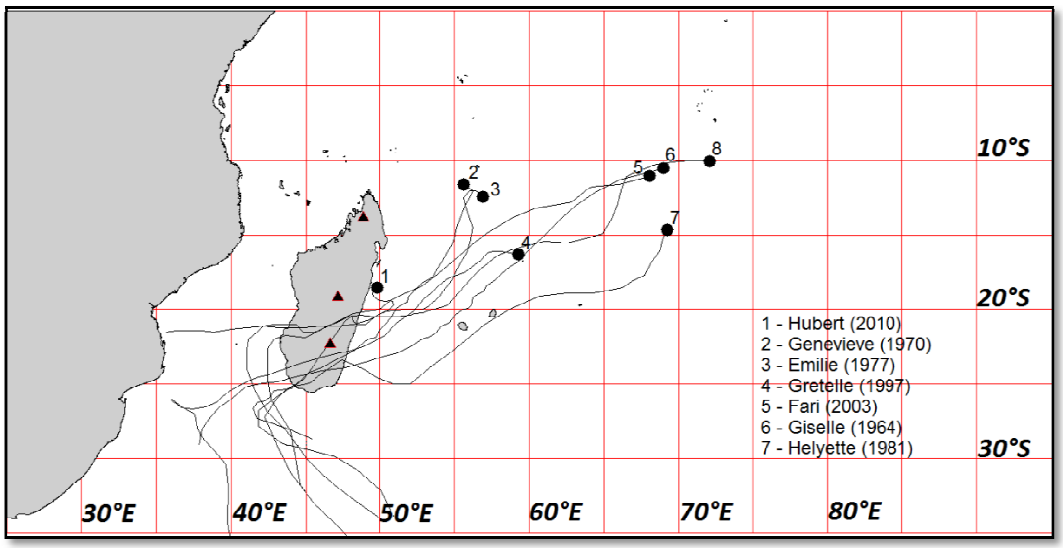

Figure 7: Type C track – Landfalling to the south of the latitude 20°S

This category (Type C) groups tropical cyclone tracks that reach the east coast of Madagascar to the south of 20°S. We can observe that the massif of Andringitra (Peak coordinates: 46.8°E / 22.2°S) may induce some northward or southward track deflections.

3.1.4 Type D Track

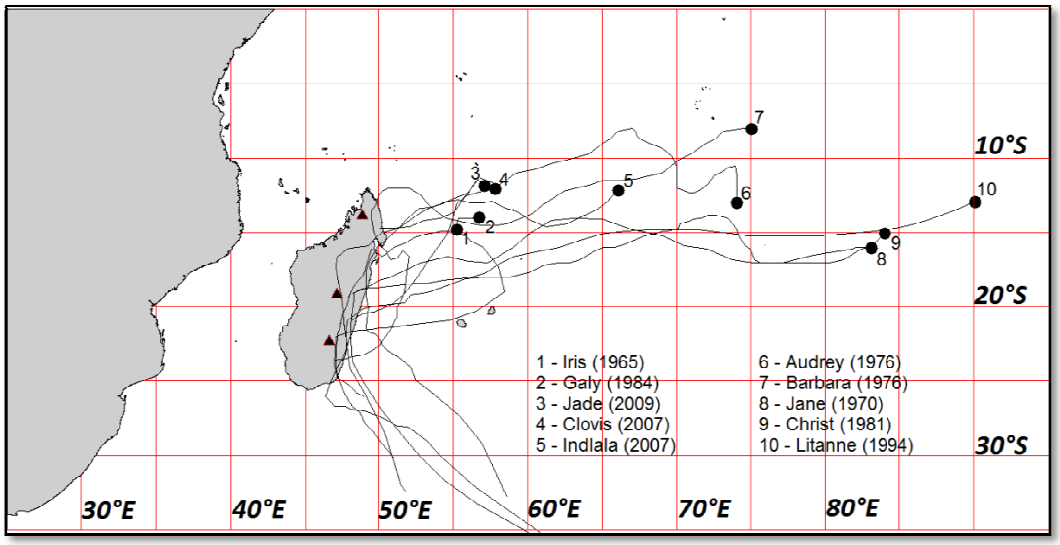

Figure 8: Type D track – Landfalling on eastern Madagascar and then curving anticyclonically back to the Indian Ocean.

Tropical cyclones belonging to this category (Type D) landfall on eastern Madagascar, but then curve back to cross the Indian Ocean. The Madagascar mountain ridge which runs north-south through the length of the island exerts a strong southward deflection on the tracks just after the landfalling.

3.1.5 Type E Track

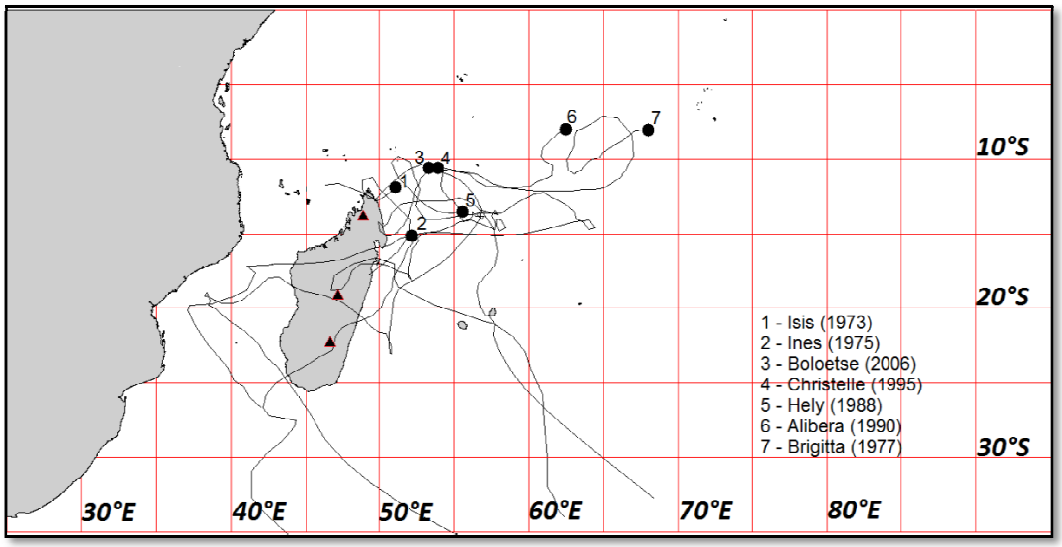

Figure 9: Type E track – looping or erratic tropical cyclone tracks.

This category groups tropical cyclones tracks that are generally atypical. They are characterized by looping before reaching the coasts. The study of the orographic effects on this track type should be done by case studies because it cannot be generalized.

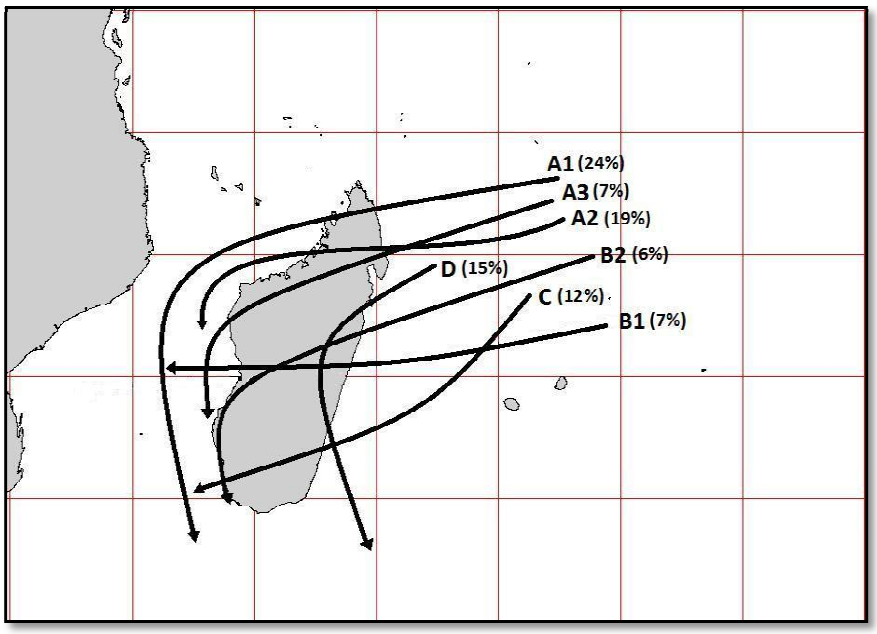

Figure 10: Summary of the classification of cyclone tracks reaching the east coast of Madagascar. (Type E is not shown)

Figure 10 generalizes the tracks classified above for cyclones reaching the east coast of Madagascar. Type A represents 50% of the total number of cyclones reaching the east coast of the island between 1963 and 2010. Type A is divided into three subcategories, A1 (24%), A2 (19%), and A3 (7%). The second half of cyclones are distributed over Types B (13%), C (12%), D (15%) and E (10%).

3.2. Variability of the Track Types

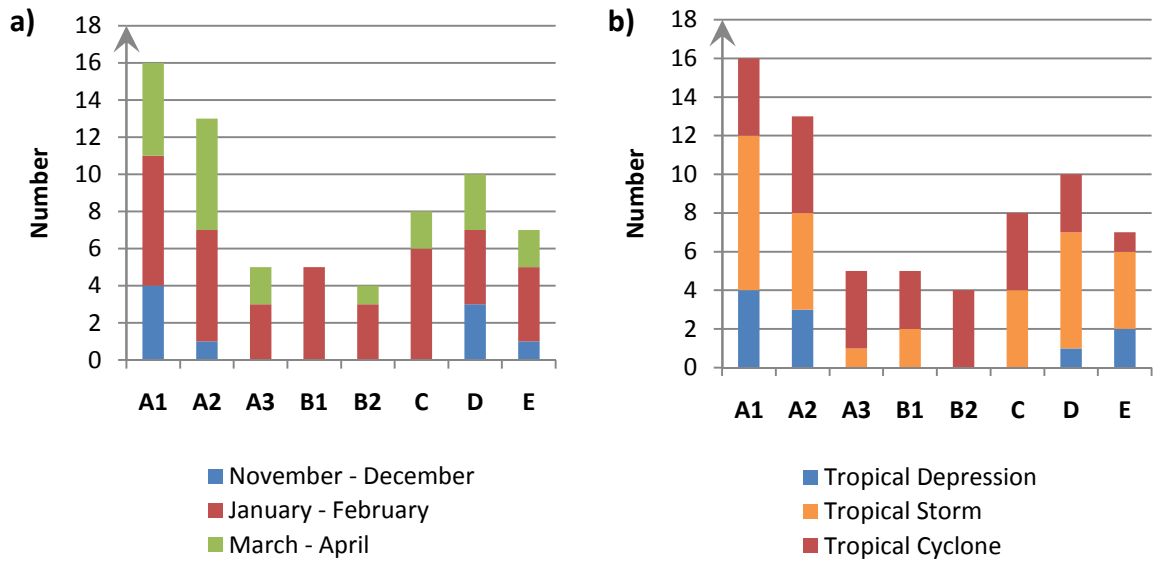

Figure 11: Variability of the Track Types. (a) Seasonal variability of the cyclone types; (b) Intensity variability during the landfalling.

Figure 11a shows that Type A1 and Type D are the most frequent during the onset of the tropical cyclone season (November – December) over Madagascar. During the peak (January – February) and the end (March – April) of the season almost all types of cyclone track occurred. However, we must note that the two first subtypes of type A are the most frequent during the end of the season (March – April).

In terms of intensity (Fig. 11b), we can notice that only the types A1, A2, D and E present tropical disturbances which do not exceed tropical depression intensity (28 – 33 Kt) during the landfalling. Conversely, all the cyclone tracks in the types A3, B1, B2 and C exceed the tropical storm intensity (33 – 63 Kt) during the landfalling. Note that almost all cyclone tracks that moves toward southwest when crossing Madagascar (Types A3 and B2) have reached tropical cyclone intensity or higher (>63 Kt) during the landfalling. This statistical observation may explain why track deflections are less apparent in the types A3 and B2. Therefore, we may propose that the orographic effects on tropical cyclone tracks are strongly influenced by their intensity and the approach angle encountering Madagascar mountain barriers.

3.3. Continuous and Discontinuous Tracks

In this part of the study, the main objective is to determine if the huge mountain barrier that is Madagascar mountain range in this case may induce a discontinuity of the cyclone track when a cyclone crosses the island. According to the several studies on the effects of the orography of Taiwan on cyclone track modification (e.g. Chang 1982; Yeh and Elsberry 1993b; Lin et al. 1999; Wu and Kuo 1999; Lin et al. 2005), when a cyclone impinges on Taiwan's mountain range, its track may remain continuous or become discontinuous.

A continuous track occurs when the cyclone simply continues its path on surface over the mountain range or when it is deflected without looping and remain for some time on the eastern side of the mountain range before crossing. On the other hand, when the path of a cyclone on the surface cannot be traced across the mountain range it is called discontinuous track. For a cyclone with discontinuous track, we hypothesize that one or more secondary lows may form over the west side of the island; One of these secondary lows eventually develops and replaces the center of the original low-level low pressure which is blocked to the east of the island.

In order to determine whether similar discontinuities may occur when a tropical cyclone crosses the Madagascar mountain range, we plotted first 6-hourly NCEP/NCAR reanalysis data composite maps of the sea level pressure of all tropical cyclones for each track type found previously. These maps were obtained from the NOAA/ESRL Climate Diagnostic Center's "6-Hourly Composites" web page (http://www.esrl.noaa.gov/psd/data/composites/hour/).

These composite maps allowed us to preliminary detect some potential cases with discontinuous tracks from the NCEP/NCAR reanalysis data which have a resolution of 2.5° x 2.5° latitude-longitude, although it is too coarse for an orographic effects study. For example, the sea level pressure composite maps for tropical cyclones Ivan (2008) and Domoina (1984) are shown in Figures 12 and 13, respectively. We can observe that the track of the cyclone Ivan (2008) is likely continuous whereas the track of the cyclone Domoina (1984) is likely discontinuous due to the formation and the development of the secondary low over the west side of Madagascar.

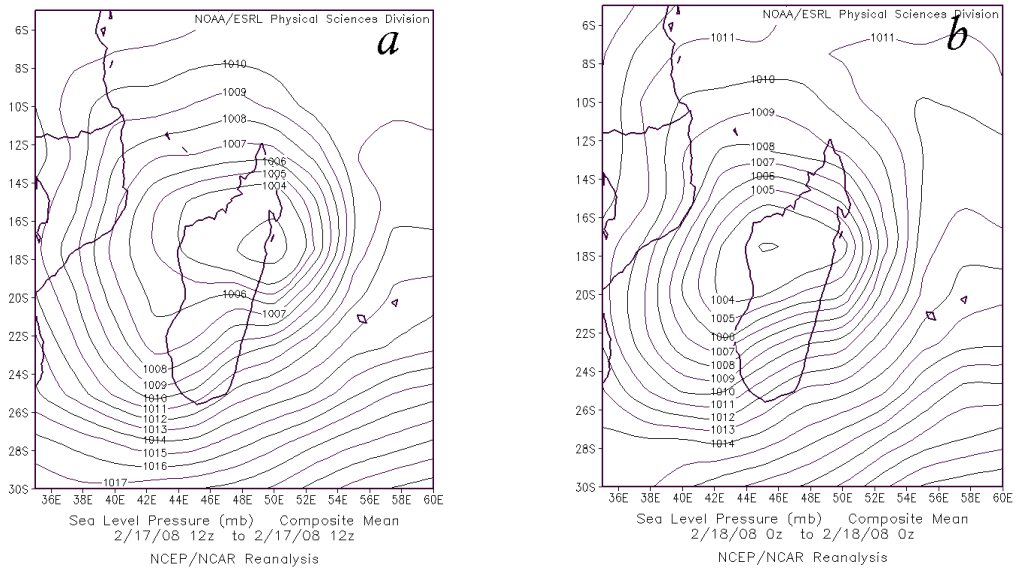

Figure 12 : Sea level pressure composite map for the cyclone Ivan (2008). (a) 12UTC/02/17/08 and (b) 00UTC/02/18/08.

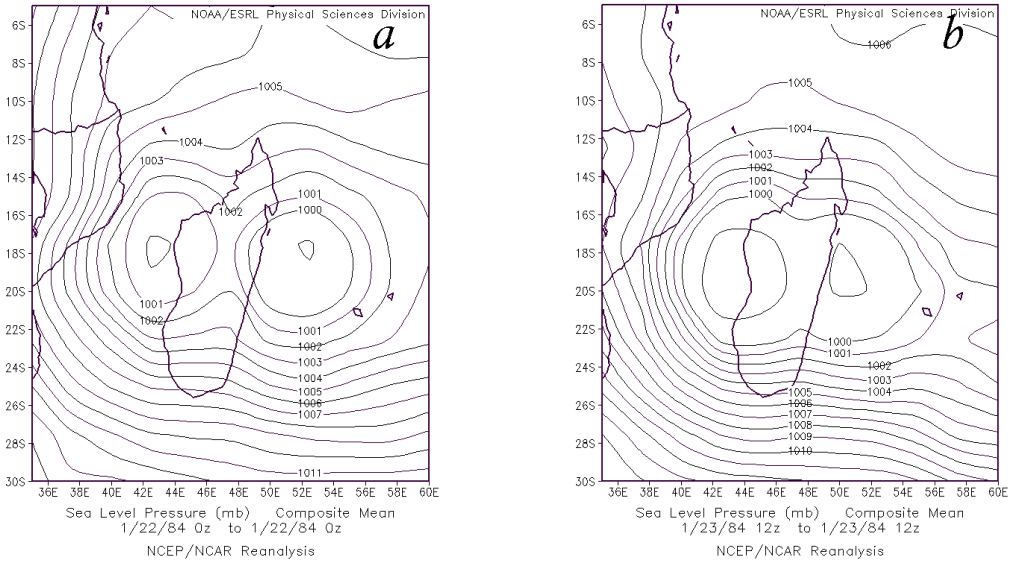

Figure 13 : Sea level pressure composite map for the cyclone Domoina (1984). (a) 00UTC/01/22/84 and (b) 12UTC/01/23/84.

Then, we chose 2 tracks from each track type in such a way that the selected tracks present a possible discontinuity of the track and a clear deflection of the track when encountering and crossing the island. In this way, we selected 16 tracks in all (Table 1).

Finally, in order to use finer-resolution data to investigate the discontinuity of the tracks, we interpolated analysis data of the global model GME of the German Weather Service (Deutscher Wetterdienst) to the High resolution Regional Model (HRM/DWD) over Madagascar within the domain of [(35.0°E, 32.5°S), (60.0°E, 7.5°S)]. The interpolated data with 14 km resolution generally serve as the initial data for HRM forecasts but here we plot them to analyze the mean sea level pressure (MSLP) and associated streamlines patterns over Madagascar as the 16 tropical cyclones approach and cross the island.

Table 1: List of the 16 selected tropical cyclones.

Type	Name	Start Date – End Date
A1	ATSRIDE	(12/28/1999 – 01/02/2000)
A1	CELA	(12/04/2003 – 12/22/2003)
A2	DOAZA	(01/22/1988 – 02/01/1988)
A2	FABRIOLA	(01/02/1997 – 01/11/1997)
A3	CALIDERA	(01/11/1988 – 01/21/1988)
A3	GLORIA	(02/27/2000 – 03/10/2000)
B1	DOMOINA	(01/16/1984 – 02/02/1984)
B1	ELINE	(02/07/2000 – 02/29/2000)
B2	HONORININA	(03/09/1986 – 03/23/1986)
B2	IVAN	(02/05/2008 – 02/27/2008)
C	FARI	(01/24/2003 – 02/02/2003)
C	GRETELLE	(01/19/1997 – 01/31/1997)
D	LITANNE	(03/07/1994 – 03/19/1994)
D	JADE	(04/03/2009 – 04/11/2009)
E	HELY	(03/16/1988 – 04/03/1988)
E	ALIBERA	(12/16/1990 – 01/07/1990)

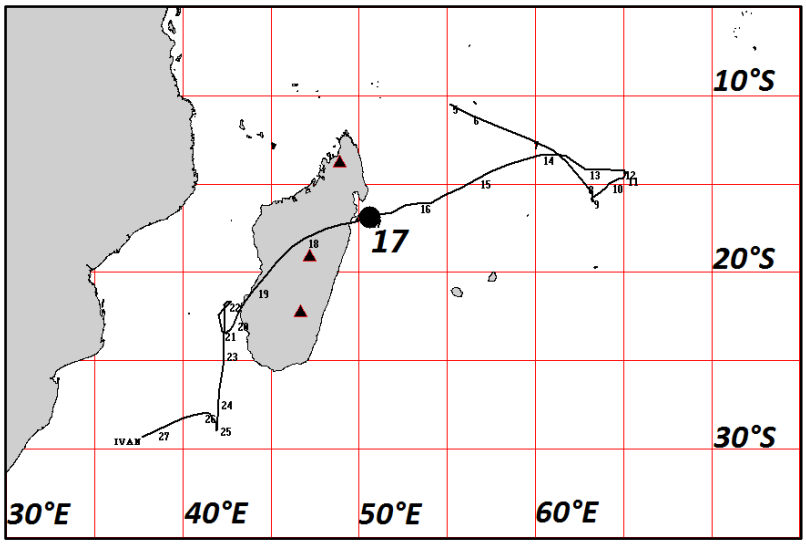

Figure 14: Track of cyclone Ivan (2008) (Type B2) for the period of 02/15/08 – 02/20/08.

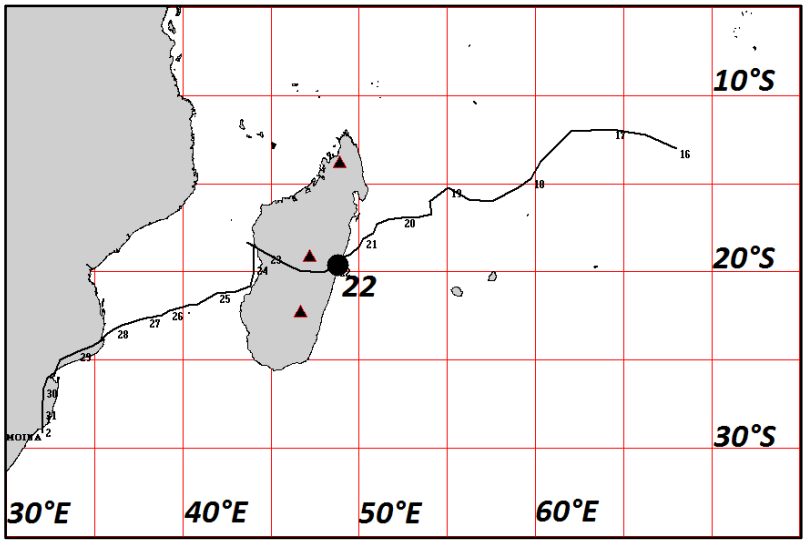

Figure 15: Track of cyclone Domoina (1984) (Type B1) for the period of 01/16/84 – 02/02/84.

Figures 14 and 15 show the best tracks of the cyclones Ivan (2008) and Domoina (1984) from the Regional Specialized Meteorological Center (RSMC) of Reunion. For the case of Ivan (2008), we plotted the mean sea level pressure (MSLP) and the streamline fields every 12h from 00UTC/02/16/08 to 12UTC/02/18/08 (Fig. 16) since the landfall occurs on 02/17/08 and for the case of Domoina (1984), we did the same for the period of 12UTC/01/21/84 to 00UTC/01/24/84 (Fig. 17) since the landfall occurs on 01/22/84. That way, we can follow the evolution of the low-level pressure center as the cyclone crosses Madagascar.

We can confirm easily the continuity of the cyclone Ivan (2008) track, since the original low-level pressure center simply continues its path over the island (Fig. 16). However, for the case of the cyclone Domoina (1984) (Fig. 17), we can notice the formation and the development of the

secondary low on the west side of the Madagascar mountain range. From 12UTC/01/21/84 (Fig. 17a) to 12UTC/01/23/84 (Fig. 17e), the original low-level pressure center remains on the eastern side of the mountain range and continue to develop slowly whereas the secondary low develops rapidly over the western side. At 00UTC/01/24/84 (Fig. 17f), the secondary low becomes the new low-level center (994 hPa) and replaces the center of the original one which weakens significantly.

Similar features can be found by looking at the associated streamlines fields. At 12UTC/ 01/22/84 (Fig. 17g) we can see a significant confluence of the circulation when the secondary center forms. Then the formation of the secondary streamline center is evident. At 00UTC/01/24/84 (Fig. 17l) the new circulation center becomes dominant and this observation confirms that the original low-level center is replaced with a new center. This process is similar to that happened in typhoons passing over Taiwan's Center Mountain Range associated with the discontinuous track (see Fig. 5.37 of Lin 2007).

Similar plots of Figs. 16 and 17 are shown in the Appendix for all the 16 cyclone tracks, but we can notice that the track of the cyclone Domoina (1984) shows the most evident discontinuity case. For type A1 and type D tracks, we note that all tracks are continuous, since there is no evidence of new centers formed on the lee side. Conversely, all tracks of types A2, A3, B1, B2, C and E seem to be discontinuous, except for Ivan (2008) track (Type B2). The continuity of its track is likely due to the weak orographic blocking that this cyclone reached before the landfalling (see the conceptual model of Lin et al. 2005 or Fig. 5.35a of Lin 2007). And among the possible discontinuous tracks, we also notice that the discontinuity of some cases like Doaza (1988) (Type A2), Fabriola (1997) (Type A2), Gloria (2000) (Type A3), Honorinina (1986) (Type B2), Hely (1988) (Type E) and Alibera (1990) (Type E) are somewhat ambiguous because the 1000 hPa streamline plots do not confirm the discontinuity observed from surface pressures fields.

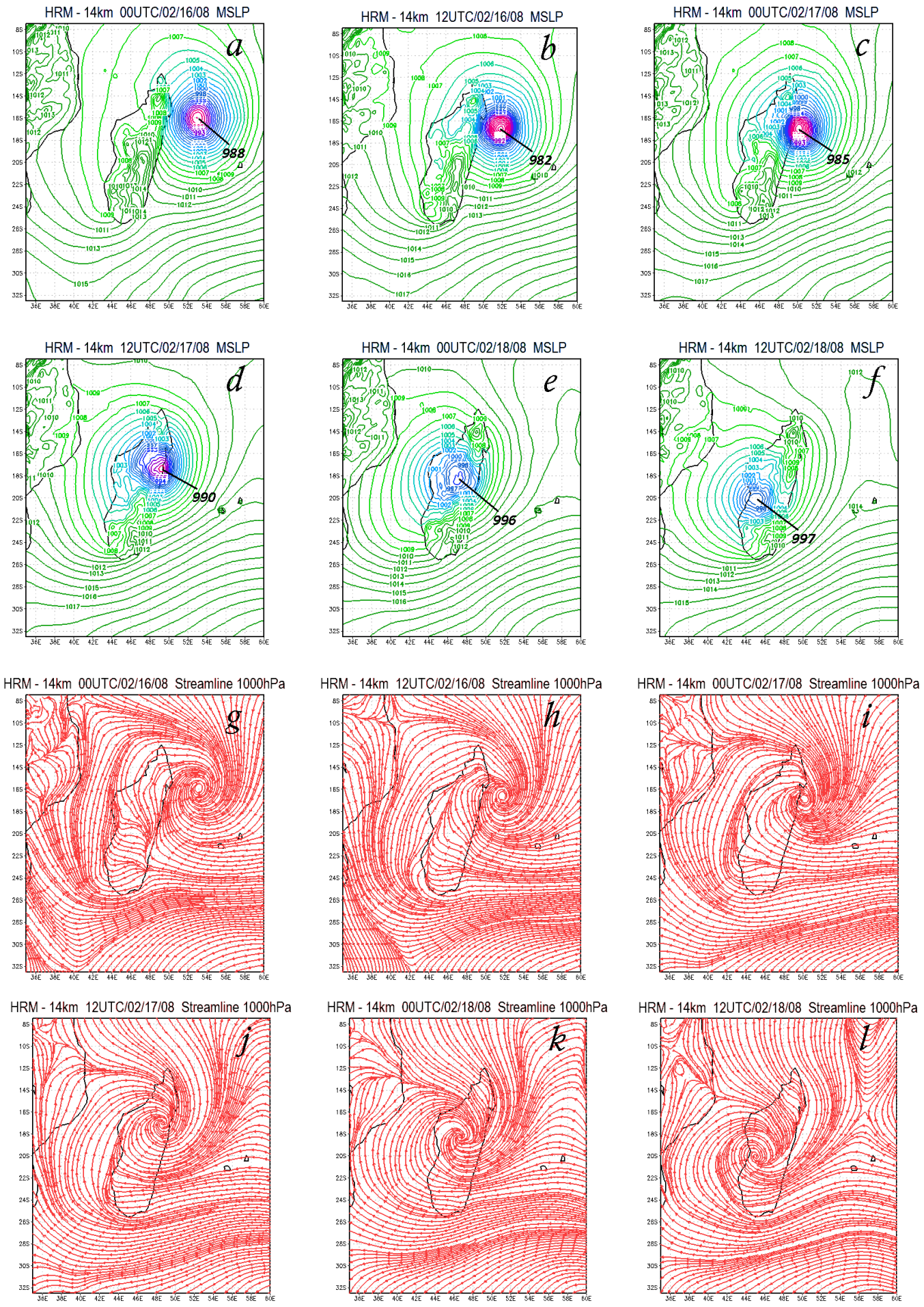

Figure 16: Mean sea level pressure (MSLP) and 1000 hPa streamline fields for cyclone Ivan (2008) (Type B2). Contour interval for the PMSL fields is 1 hPa. Each map is plotted every 12h from 00UTC/02/16/08 to 12UTC/02/18/08.

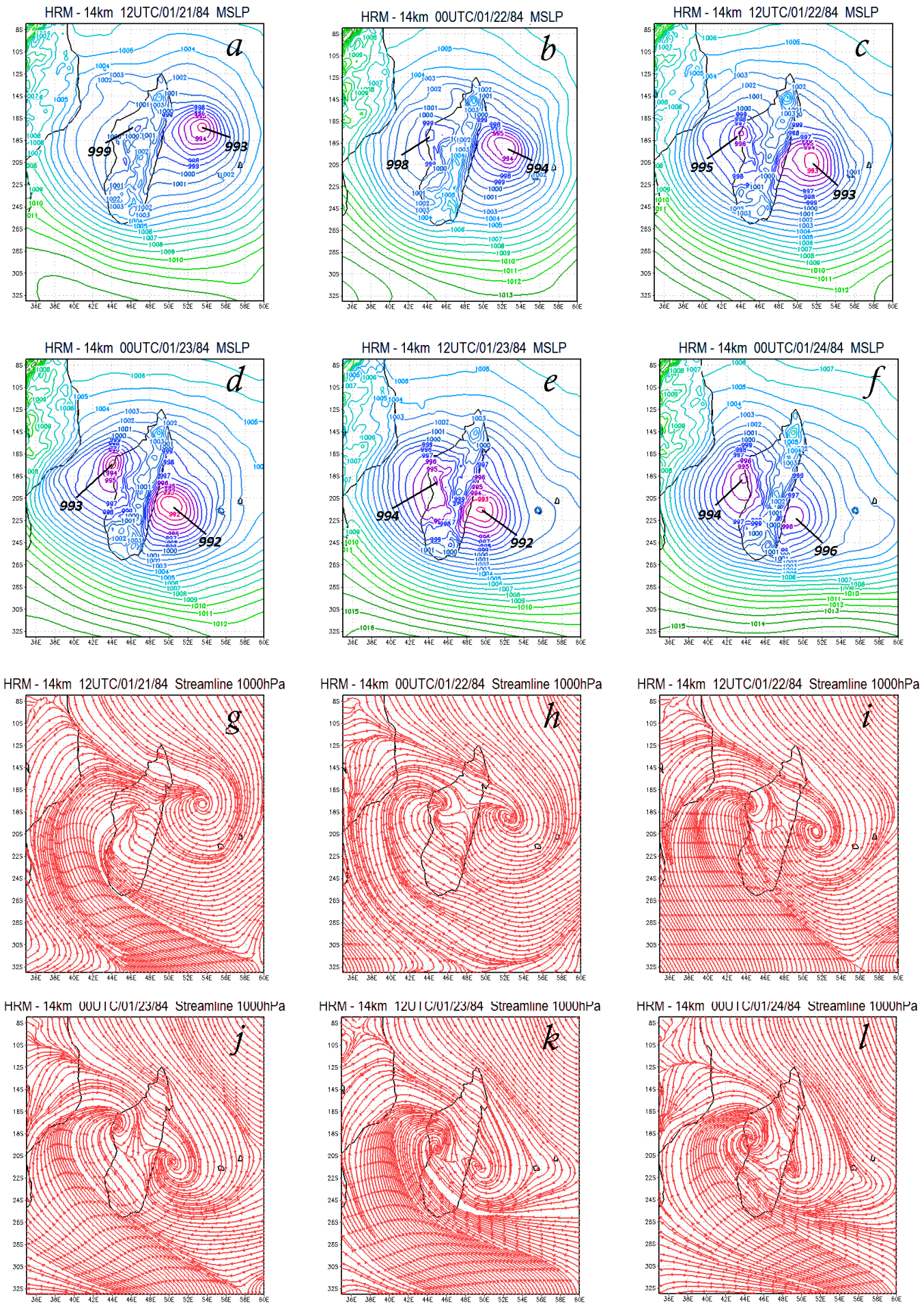

Figure 17: Mean sea level pressure (MSLP) and 1000 hPa streamline fields for cyclone Domoina (1984) (Type B1). Contour interval for the PMSL fields is 1 hPa. Each map is plotted every 12h from 12UTC/01/21/84 to 00UTC/01/24/84.

4. Conclusion

The preliminary results presented in this study show that the tropical cyclone tracks reaching the east coast of Madagascar can be classified in five major categories according to the landfall location and the way the tropical cyclone crosses the island. This classification is closely linked with the Madagascar mountain range, and particularly with the three main massifs with height above 2600 m.

Furthermore, since the Madagascar mountain ridge runs north-south through the length of the island, westward moving tropical cyclones behavior can be considerably influenced. In this way, we can observe northward and southward deflections near the peaks of the massifs.

Concerning the discontinuity of tracks when the cyclone center crosses the island, we found that among the 16 tracks we have chosen, 11 were found to be discontinuous. Except for the types A1 and D, the Madagascar's mountain range may induce a discontinuity of the cyclone track for all the track types that we have defined. These exceptions are likely due to the landfall locations of the type A1 tracks that are in the northern tip of the island and the fact that type D tracks move almost parallel to the Madagascar mountain ridge as they landfall. This confirms that in addition to intensity, the landfall location and the approach angle complicate orographic effects (Lin and Savage 2011).

Based on the preliminary results found here, we believe that there is still a lot to do in this investigation of the effects of Madagascar mountain range on tropical cyclone tracks. This initial study may be extended to identify some parameters that explain the effects of orography to the continuity and deflection of cyclone tracks (Lin et al., 2005). Finding relations between these control parameters and track behaviors is an interesting and difficult research area worthy of further exploration.

5. References

- Bender, M. A., R. E. Tuleya, and Y. Kurihara, 1987: A numerical study of the effect of island terrain on tropical cyclones. *Mon. Wea. Rev.,* ***115,*** 130–155.
- Brand, S., and J. W. Blelloch, 1974: Changes in the characteristics of typhoons crossing the island of Taiwan. *Mon. Wea. Rev.,* ***102,*** 708–713.
- Chang, S. W.-J., 1982: The orographic effects induced by an island mountain range on propagating tropical cyclones. *Mon. Wea. Rev.,* ***110,*** 1255–1270.
- Lin, Y.-L., 2007: *Mesoscale Dynamics*. Cambridge University Press, 630pp.
- Lin, Y.-L., and L. Crossby Savage III, 2011: Effects of landfalling location and the approach angle of a cyclone vortex encountering a mesoscale mountain range. *J. Atmos. Sci.,* ***68,*** 2096–2016.
- Lin, Y.-L., J. Han, D. W. Hamilton, and C.-Y. Huang, 1999: Orographic influence on a drifting cyclone. *J. Atmos. Sci.,* ***56,*** 534–562.
- Lin, Y.-L., D. B. Ensley, S. Chiao, and C.-Y. Huang, 2002: Orographic influences on rainfall and track deflection associated with the passage of a tropical cyclone. *Mon. Wea. Rev.,* ***130,*** 2929– 2950.

- Lin, Y.-L., S.-Y. Chen, C. M. Hill, and C.-Y. Huang, 2005: Control parameters for the influence of a mesoscale mountain range on cyclone track continuity and deflection. *J. Atmos. Sci.,* ***62,*** 1849–1866.
- Lin, Y.-L., N. C. Witcraft, and Y.-H. Kuo, 2006: Dynamics of Track Deflection Associated with the Passage of Tropical Cyclones over a Mesoscale Mountain. *Mon. Wea. Rev.,* ***134,*** 3509–3538.
- Wu, C.-C., and Y.-H. Kuo, 1999: Typhoons affecting Taiwan: Current Understanding and future Challenges. *Bull. Of the AMS.* ***80***, 67-80.
- Yeh, T.-C., and R. L. Elsberry, 1993a: Interaction of typhoons with the Taiwan orography. Part I: Upstream track deflections. *Mon. Wea. Rev.,* ***121***, 3193–3212.
- Yeh, T.-C., and R. L. Elsberry, 1993b: Interaction of typhoons with the Taiwan orography. Part II: Continuous and discontinuous tracks across the island. *Mon. Wea. Rev.,* ***121***, 3213–3233.

Appendix

Type A1 - ASTRIDE

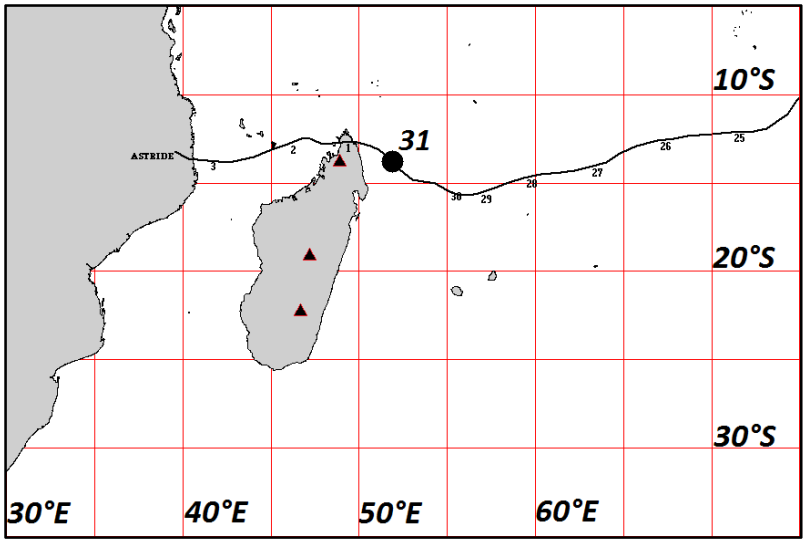

Track of cyclone ASTRIDE
(12/28/1999 – 01/02/2000)

Type A1 - CELA

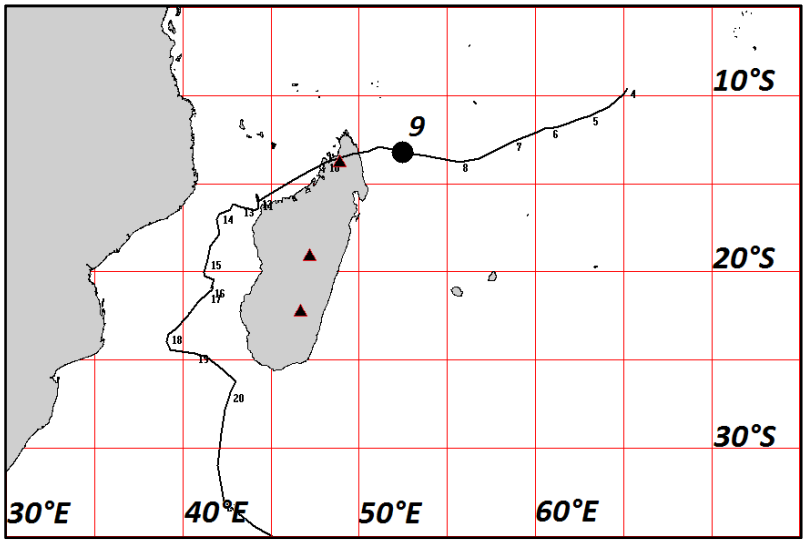

Track of cyclone CELA
(12/04/2003 – 12/22/2003)

HRM - 14km 00UTC/12/31/99 MSLP

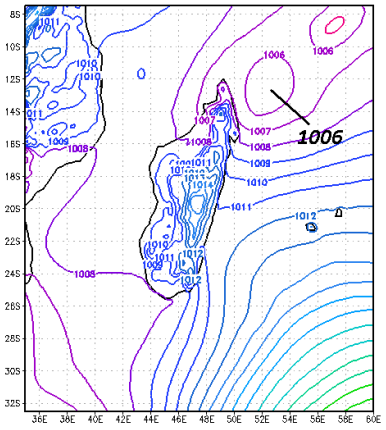

HRM - 14km 12UTC/12/31/99 MSLP

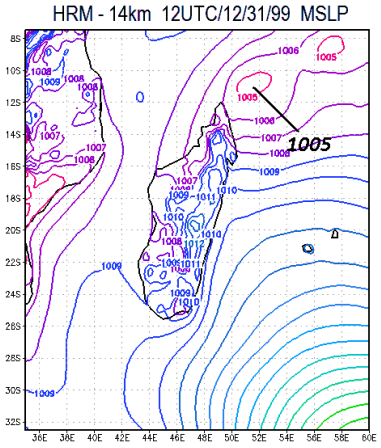

HRM - 14km 00UTC/01/01/00 MSLP

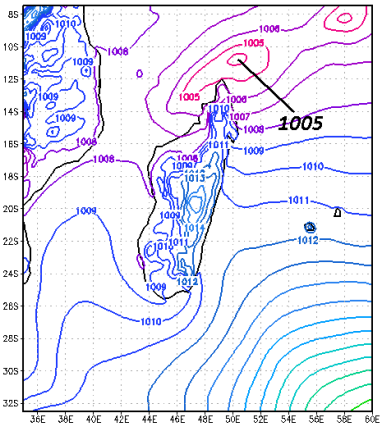

HRM - 14km 12UTC/01/01/00 MSLP

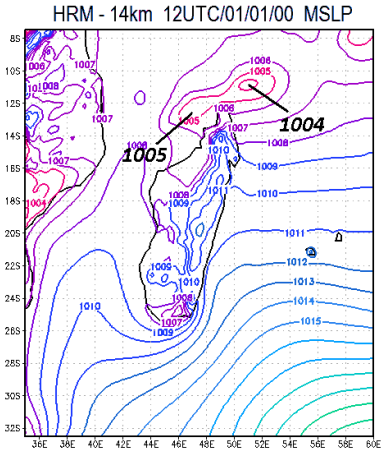

HRM - 14km 00UTC/01/02/00 MSLP

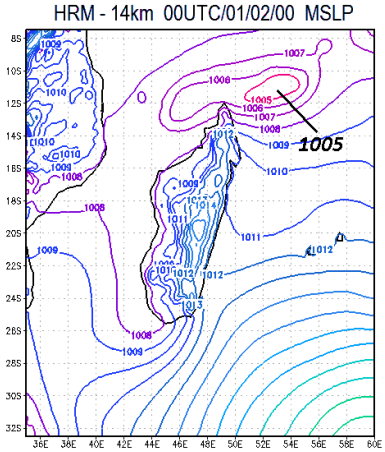

HRM - 14km 12UTC/01/02/00 MSLP

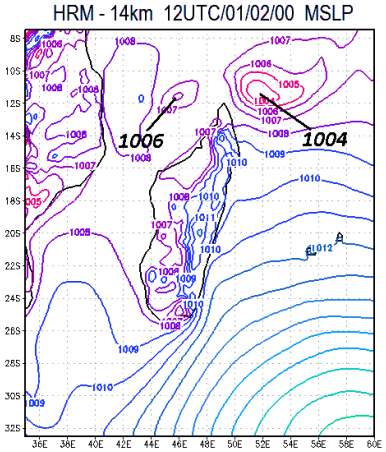

HRM - 14km 00UTC/12/31/99 Streamline 1000hPa

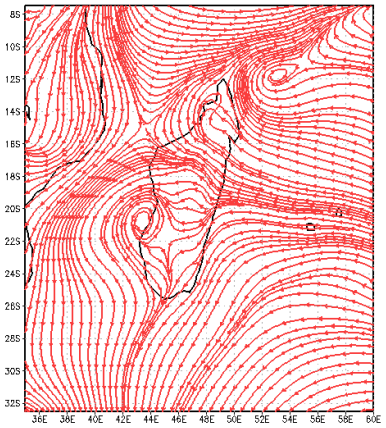

HRM - 14km 12UTC/12/31/99 Streamline 1000hPa

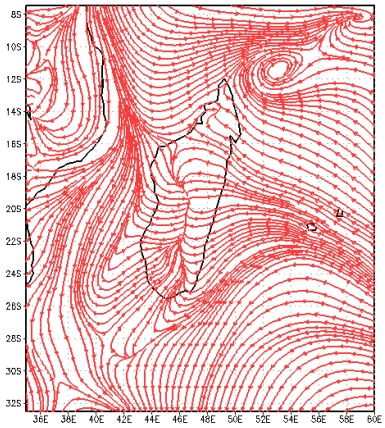

HRM - 14km 00UTC/01/01/00 Streamline 1000hPa

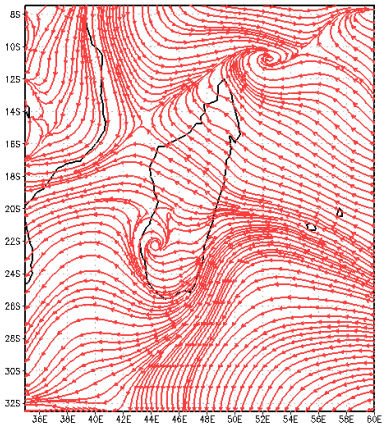

HRM - 14km 12UTC/01/01/00 Streamline 1000hPa

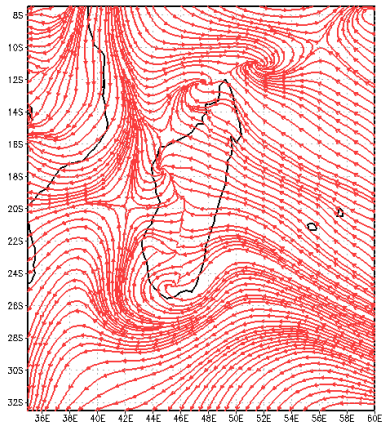

HRM - 14km 00UTC/01/02/00 Streamline 1000hPa

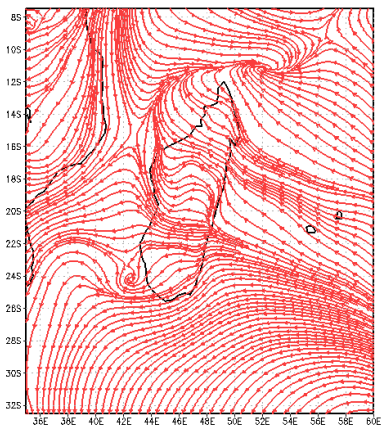

HRM - 14km 12UTC/01/02/00 Streamline 1000hPa

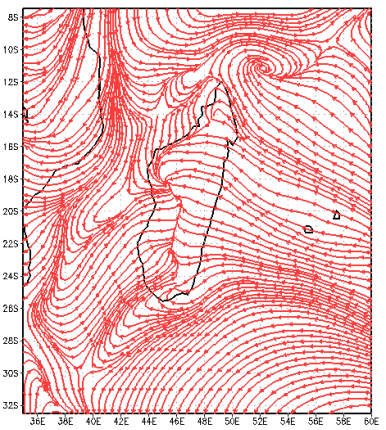

Type A1 - ASTRIDE

HRM - 14km 00UTC/12/08/03 MSLP

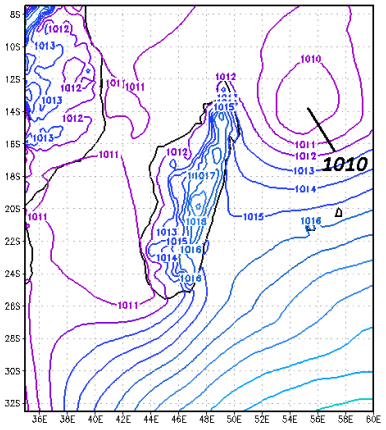

HRM - 14km 12UTC/12/08/03 MSLP

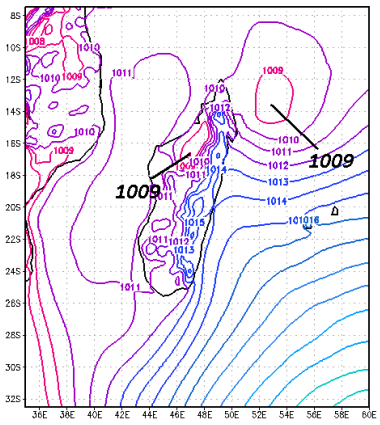

HRM - 14km 00UTC/12/09/03 MSLP

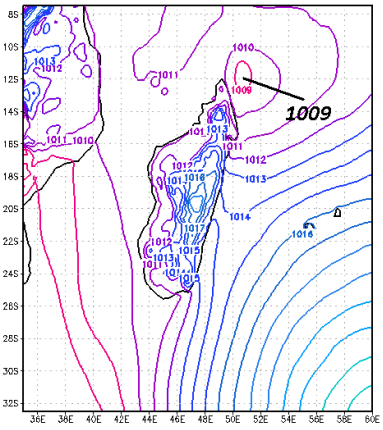

HRM - 14km 12UTC/12/09/03 MSLP

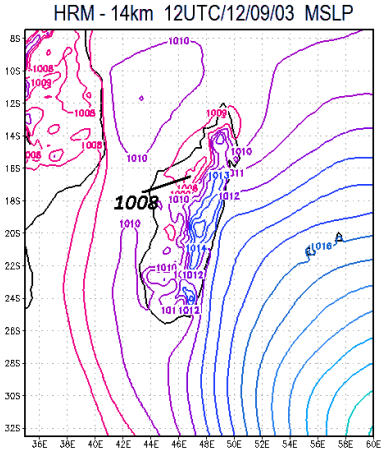

HRM - 14km 00UTC/12/10/03 MSLP

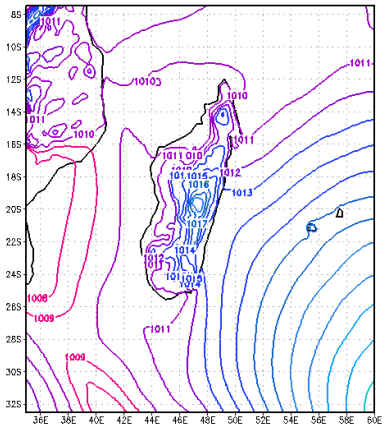

HRM - 14km 12UTC/12/10/03 MSLP

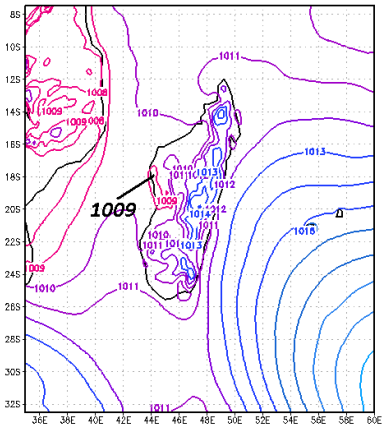

HRM - 14km 00UTC/12/08/03 Streamline 1000hPa

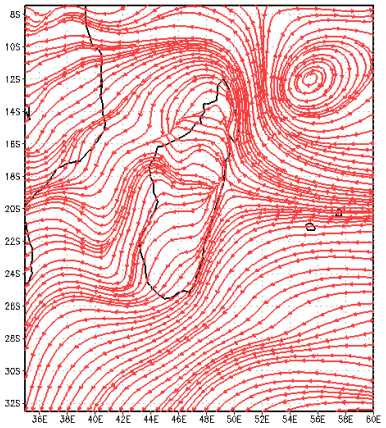

HRM - 14km 12UTC/12/08/03 Streamline 1000hPa

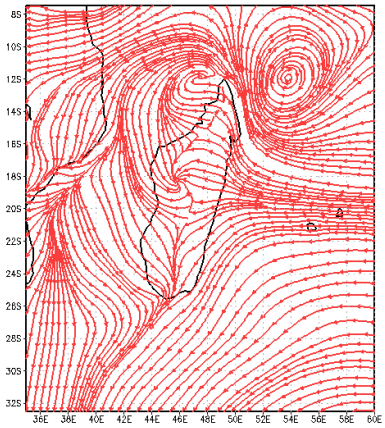

HRM - 14km 00UTC/12/09/03 Streamline 1000hPa

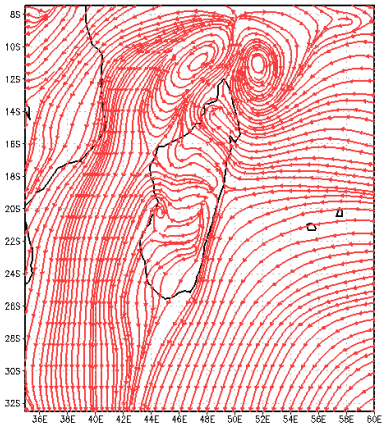

HRM - 14km 12UTC/12/09/03 Streamline 1000hPa

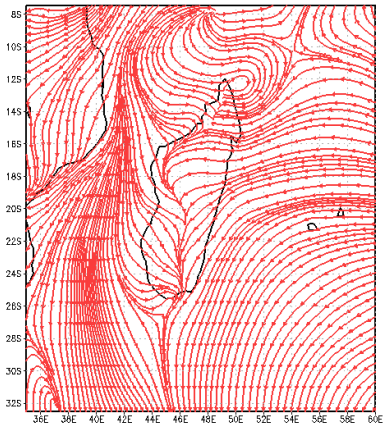

HRM - 14km 00UTC/12/10/03 Streamline 1000hPa

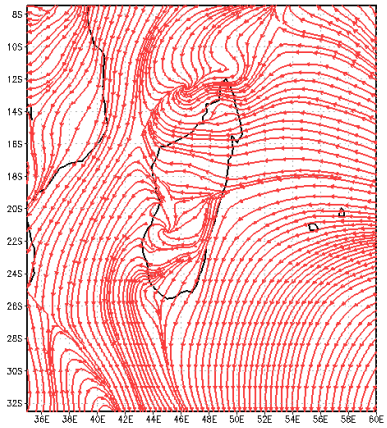

HRM - 14km 12UTC/12/10/03 Streamline 1000hPa

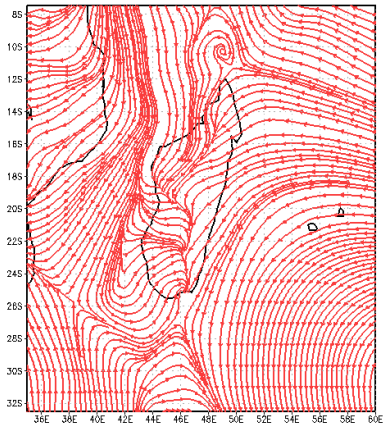

Type A1 - CELA

Type A2 - DOAZA

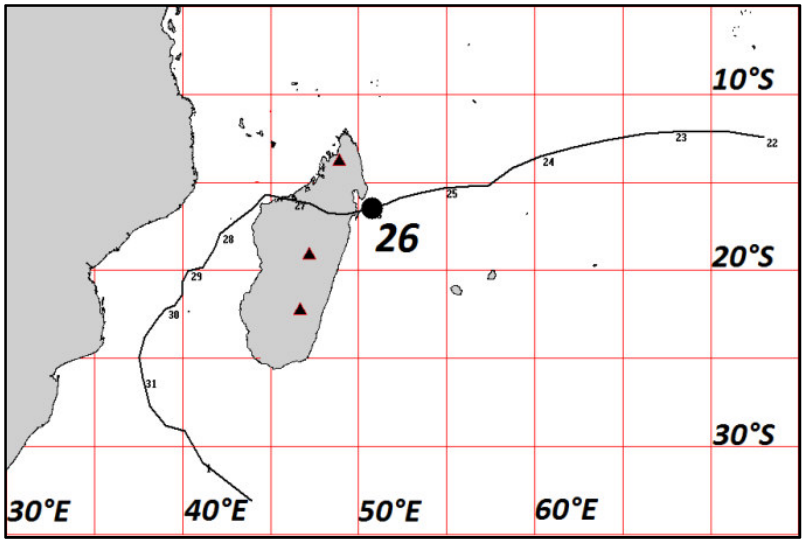

Track of cyclone DOAZA
(01/22/1988 – 02/01/1988)

Type A2 - FABRIOLA

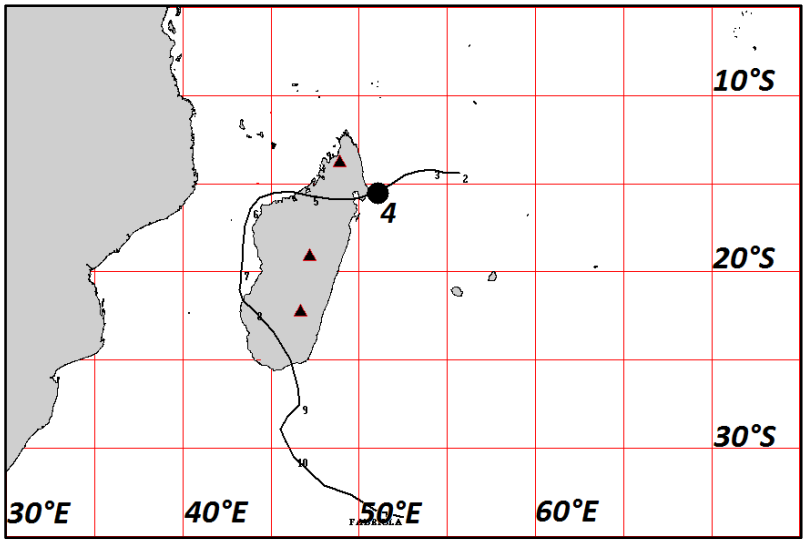

Track of cyclone FABRIOLA
(01/02/1997 – 01/11/1997)

HRM - 14km 00UTC/01/25/88 MSLP

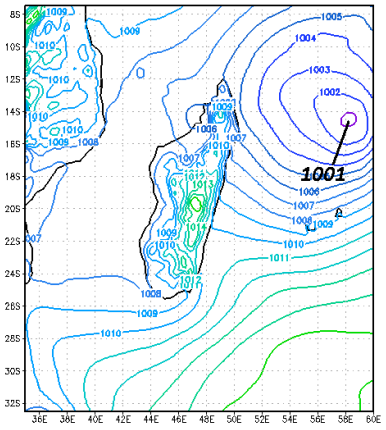

HRM - 14km 12UTC/01/25/88 MSLP

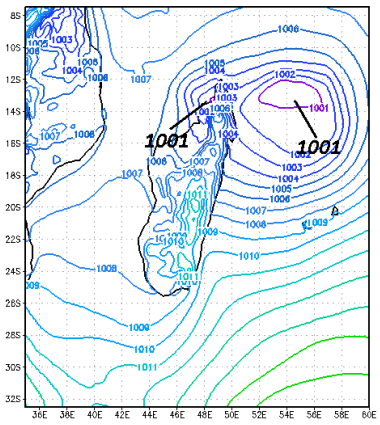

HRM - 14km 00UTC/01/26/88 MSLP

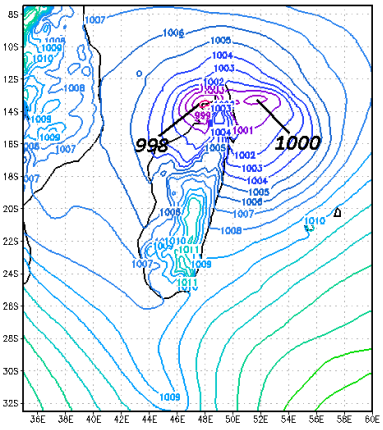

HRM - 14km 12UTC/01/26/88 MSLP

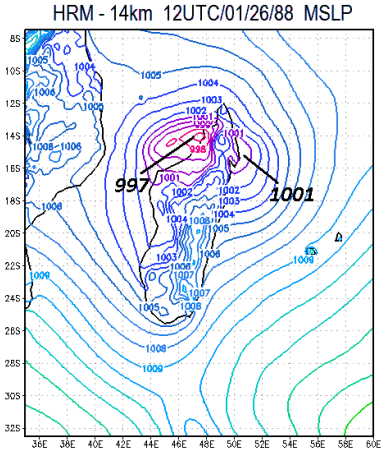

HRM - 14km 00UTC/01/27/88 MSLP

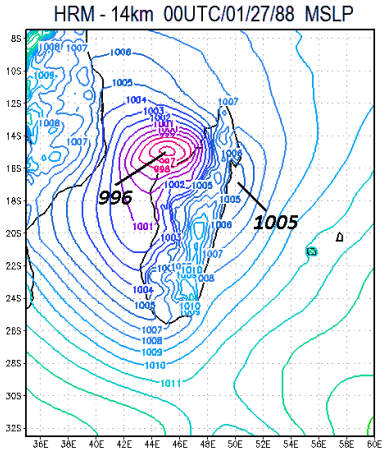

HRM - 14km 12UTC/01/27/88 MSLP

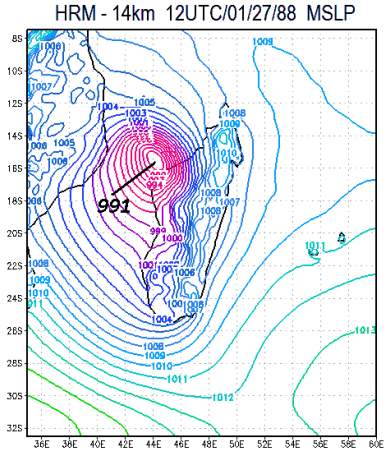

HRM - 14km 00UTC/01/25/88 Streamline 1000hPa

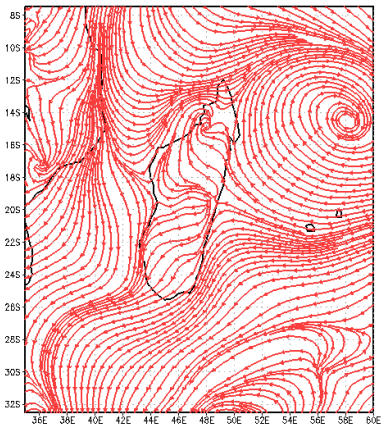

HRM - 14km 12UTC/01/25/88 Streamline 1000hPa

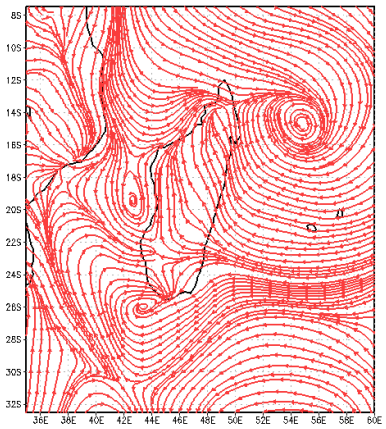

HRM - 14km 00UTC/01/26/88 Streamline 1000hPa

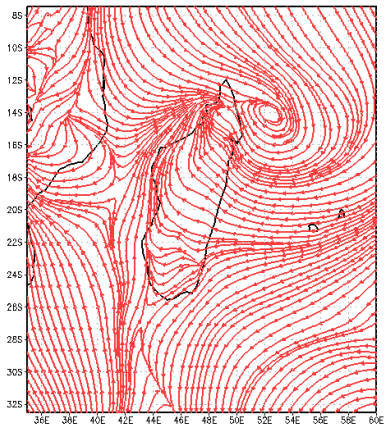

HRM - 14km 12UTC/01/26/88 Streamline 1000hPa

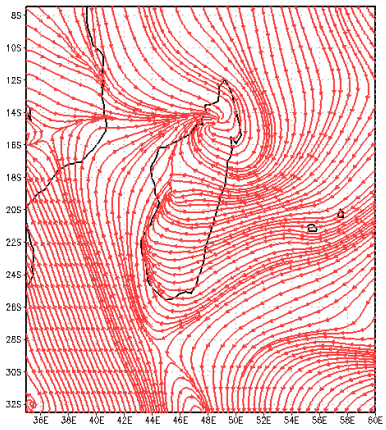

HRM - 14km 00UTC/01/27/88 Streamline 1000hPa

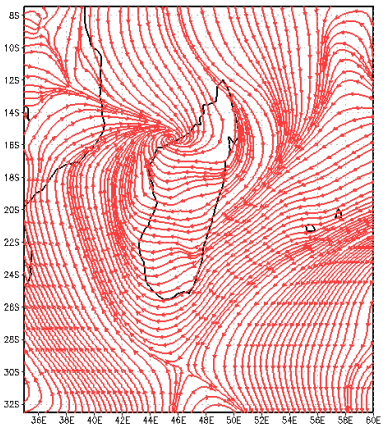

HRM - 14km 12UTC/01/27/88 Streamline 1000hPa

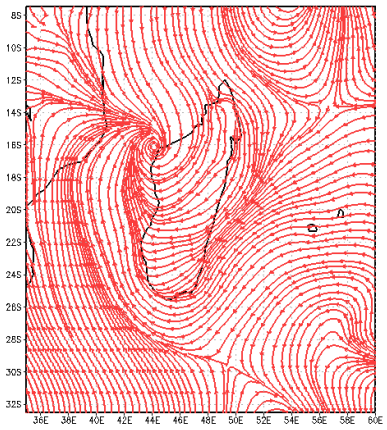

Type A2 - DOAZA

HRM - 14km 00UTC/01/03/97 MSLP

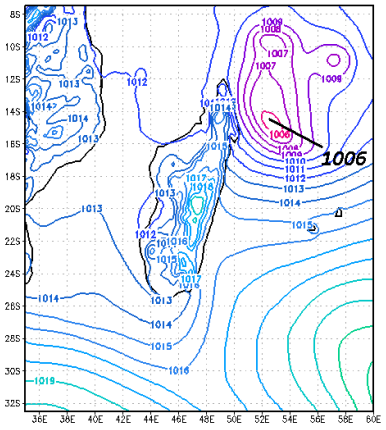

HRM - 14km 12UTC/01/03/97 MSLP

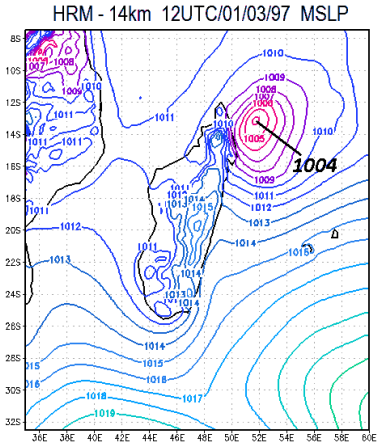

HRM - 14km 00UTC/01/04/97 MSLP

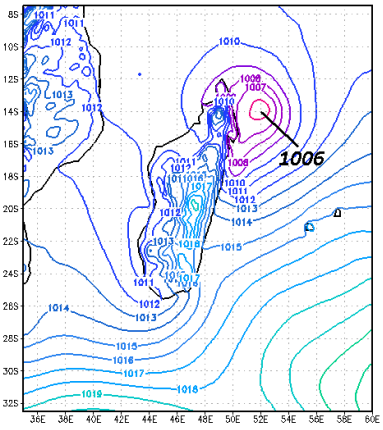

HRM - 14km 12UTC/01/04/97 MSLP

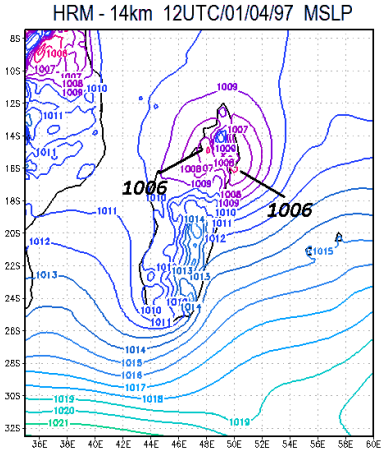

HRM - 14km 00UTC/01/05/97 MSLP

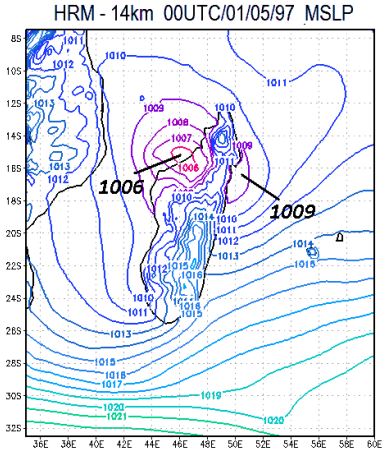

HRM - 14km 12UTC/01/05/97 MSLP

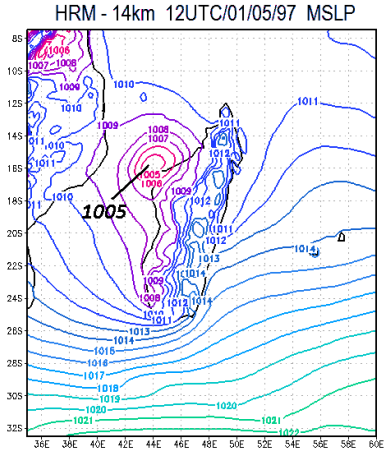

HRM - 14km 00UTC/01/03/97 Streamline 1000hPa

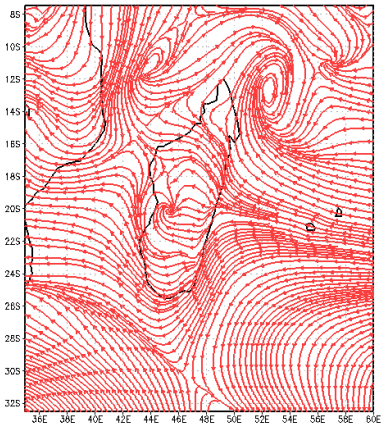

HRM - 14km 12UTC/01/03/97 Streamline 1000hPa

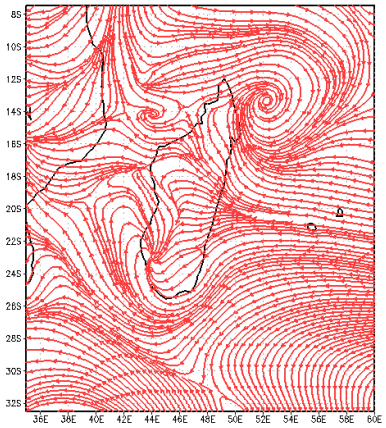

HRM - 14km 00UTC/01/04/97 Streamline 1000hPa

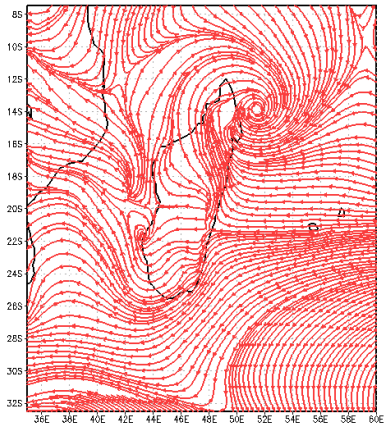

HRM - 14km 12UTC/01/04/97 Streamline 1000hPa

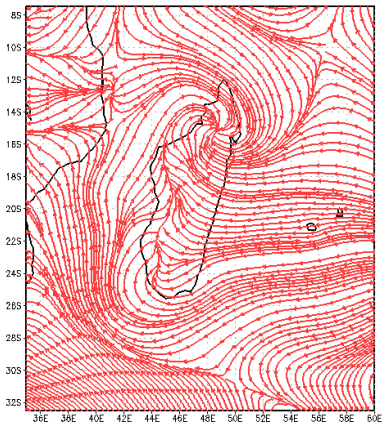

HRM - 14km 00UTC/01/05/97 Streamline 1000hPa

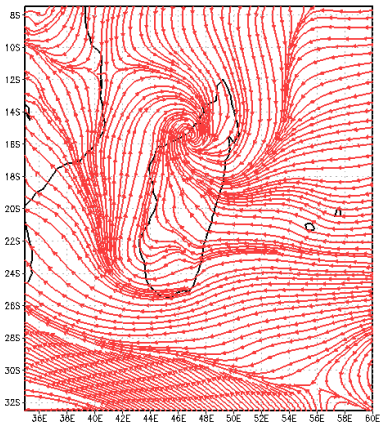

HRM - 14km 12UTC/01/05/97 Streamline 1000hPa

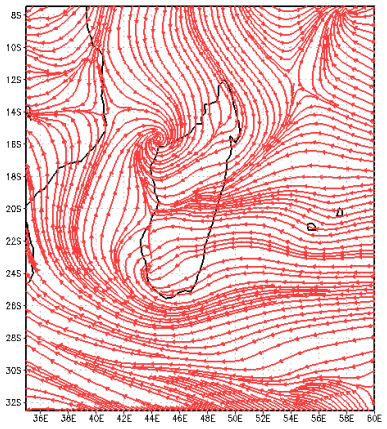

Type A2 - FABRIOLA

Type A3 - CALIDERA

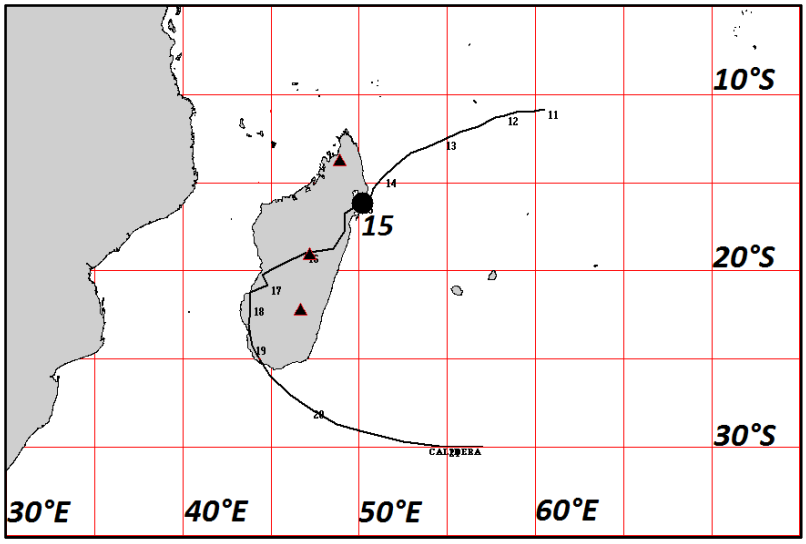

Track of cyclone CALIDERA
(01/11/1988 – 01/21/1988)

Type A3 - GLORIA

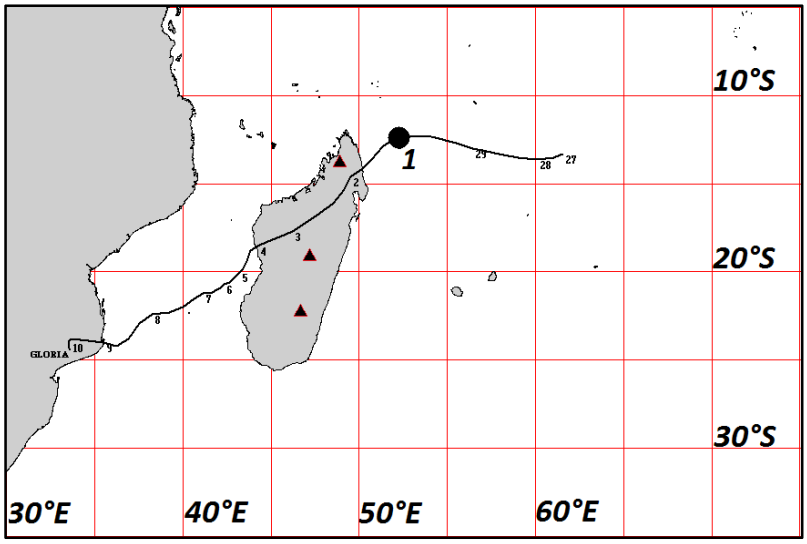

Track of cyclone GLORIA
(02/27/2000 – 03/10/2000)

HRM - 14km 00UTC/01/15/88 MSLP

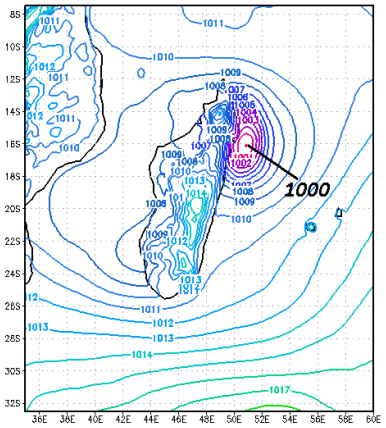

HRM - 14km 12UTC/01/15/88 MSLP

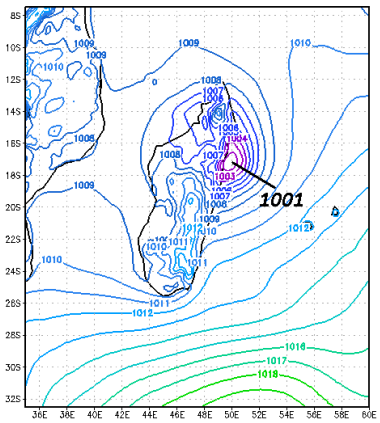

HRM - 14km 00UTC/01/16/88 MSLP

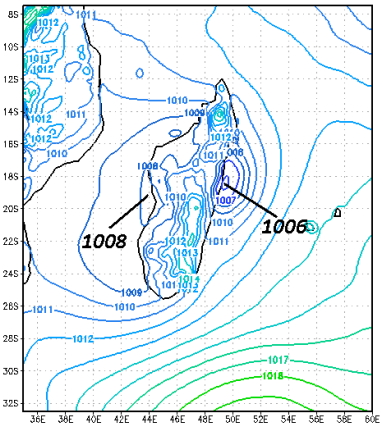

HRM - 14km 12UTC/01/16/88 MSLP

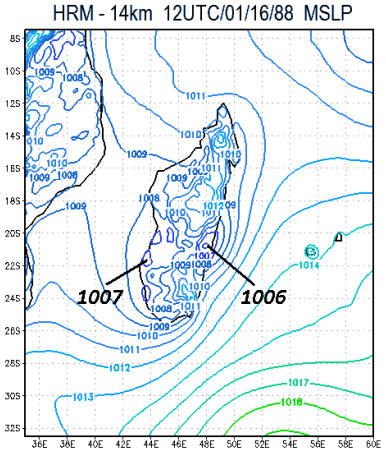

HRM - 14km 00UTC/01/17/88 MSLP

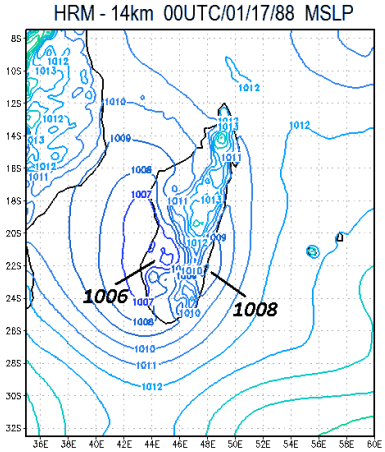

HRM - 14km 12UTC/01/17/88 MSLP

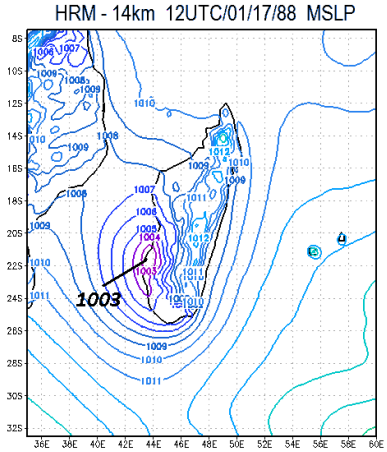

HRM - 14km 00UTC/01/15/88 Streamline 1000hPa

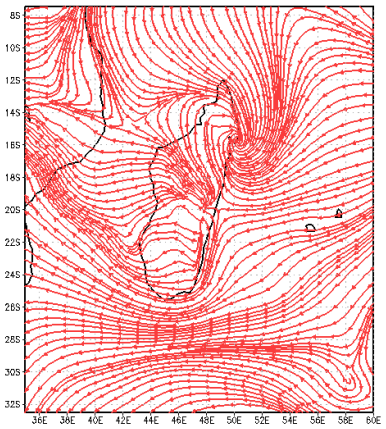

HRM - 14km 12UTC/01/15/88 Streamline 1000hPa

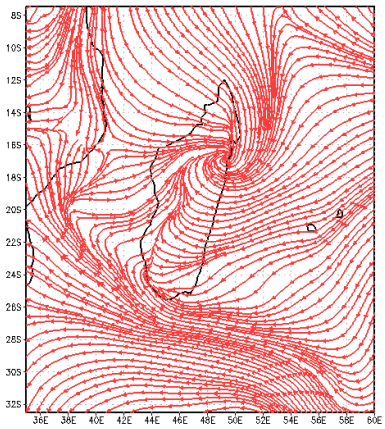

HRM - 14km 00UTC/01/16/88 Streamline 1000hPa

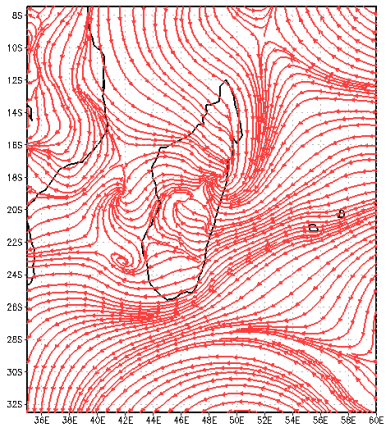

HRM - 14km 12UTC/01/16/88 Streamline 1000hPa

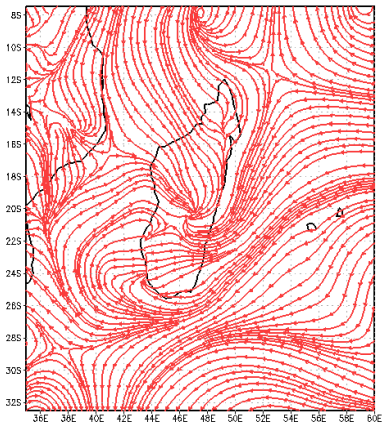

HRM - 14km 00UTC/01/17/88 Streamline 1000hPa

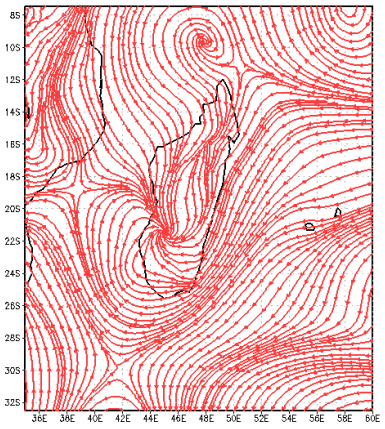

HRM - 14km 12UTC/01/17/88 Streamline 1000hPa

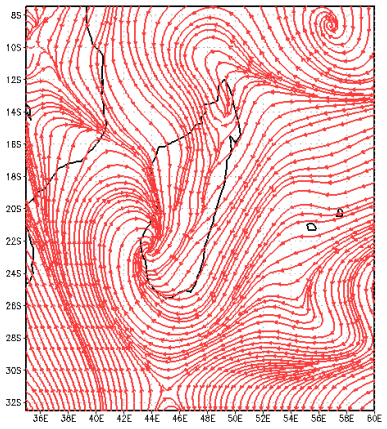

Type A3 - CALIDERA

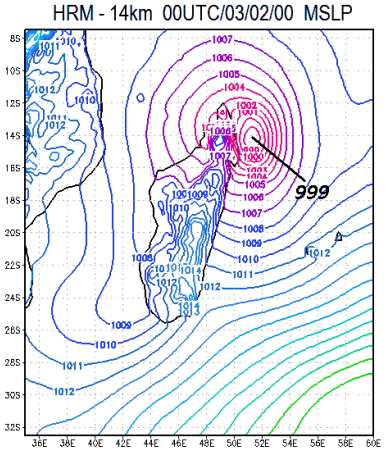

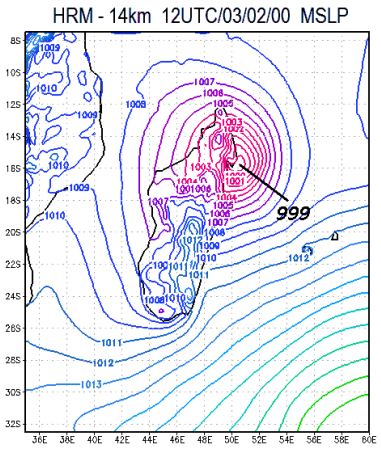

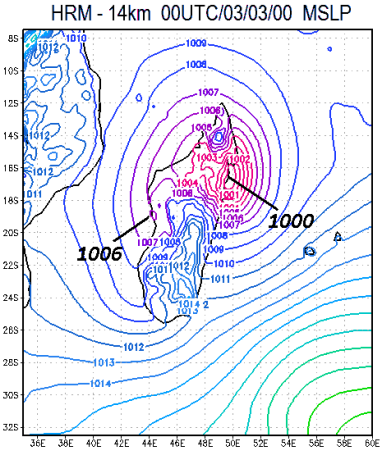

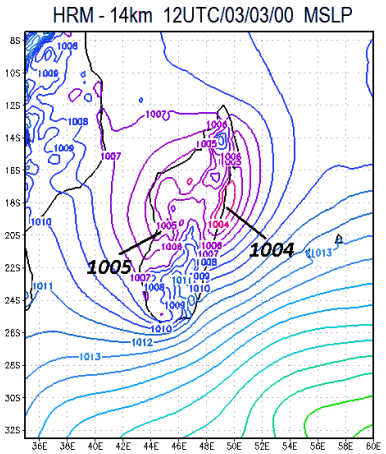

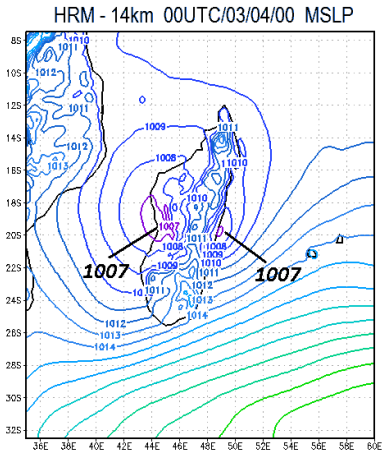

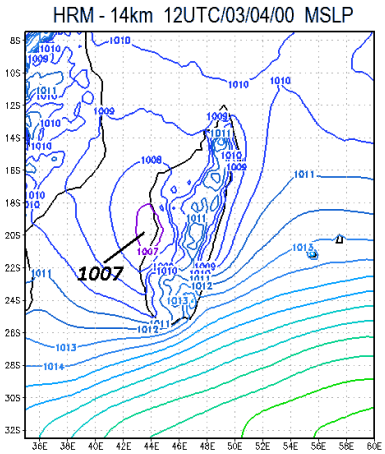

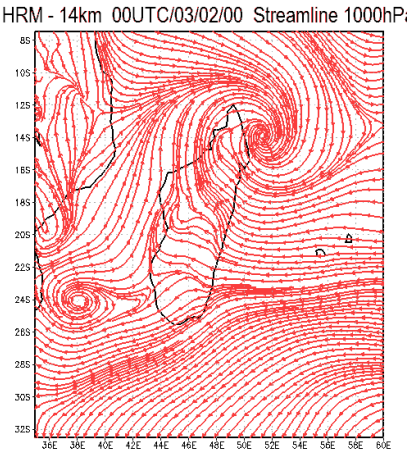

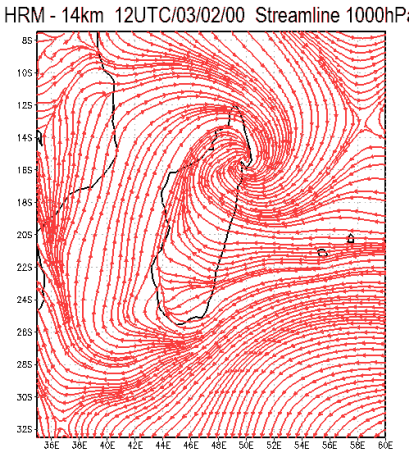

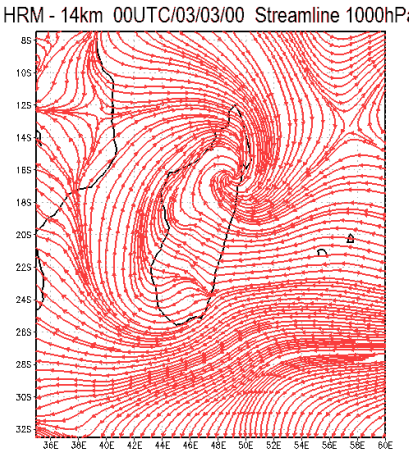

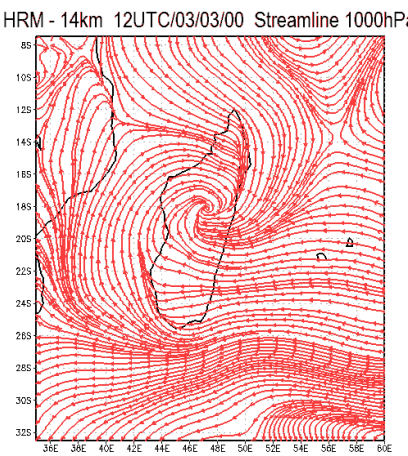

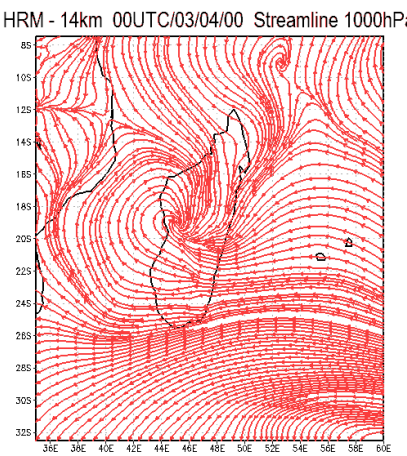

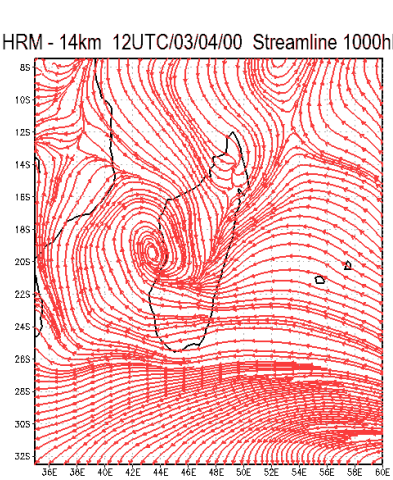

Type A3 - GLORIA

Type B1 - DOMOINA

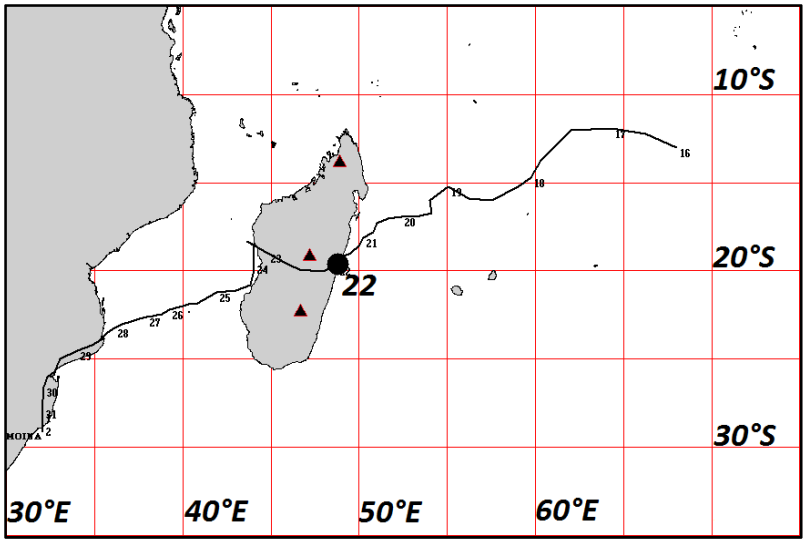

Track of cyclone DOMOINA
(01/16/1984 – 02/02/1984)

Type B1 - ELINE

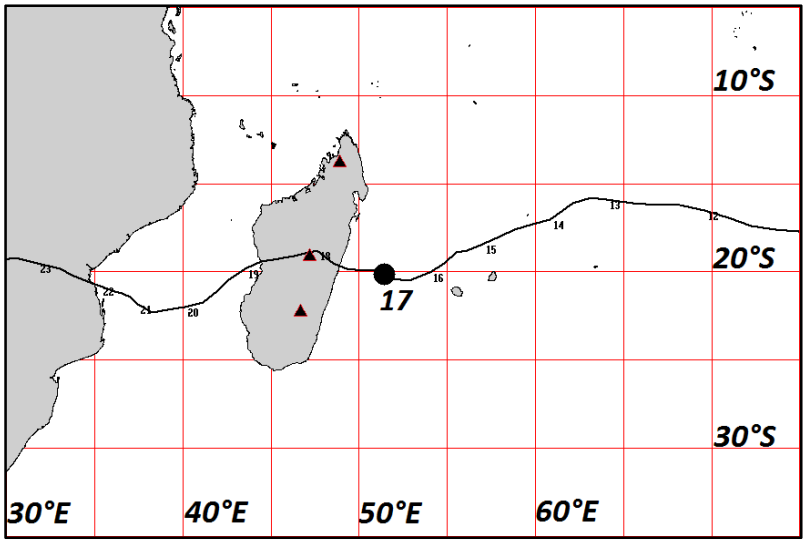

Track of cyclone ELINE
(02/07/2000 – 02/29/2000)

HRM - 14km 12UTC/01/21/84 MSLP

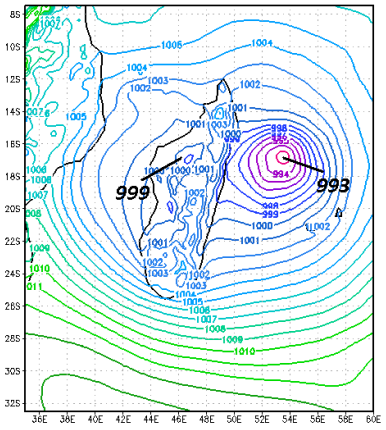

HRM - 14km 00UTC/01/22/84 MSLP

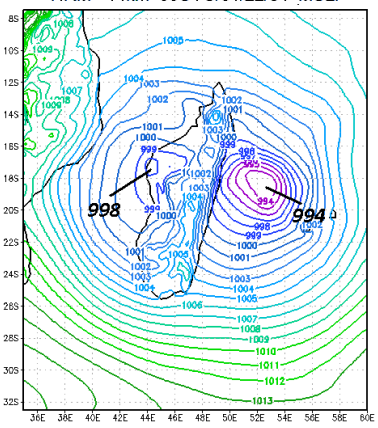

HRM - 14km 12UTC/01/22/84 MSLP

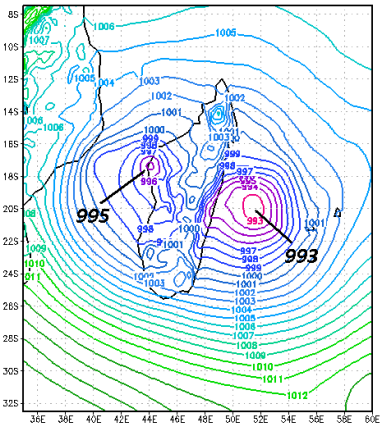

HRM - 14km 00UTC/01/23/84 MSLP

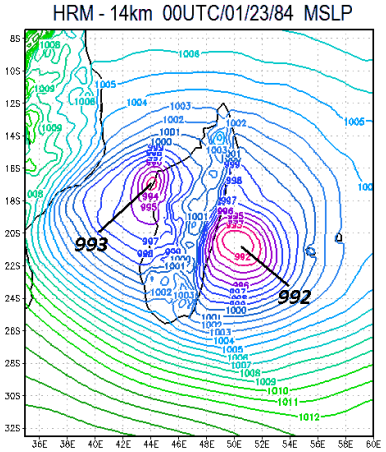

HRM - 14km 12UTC/01/23/84 MSLP

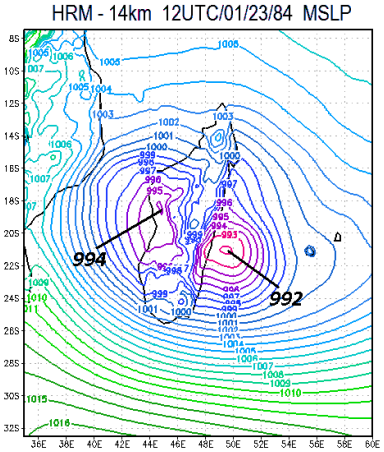

HRM - 14km 00UTC/01/24/84 MSLP

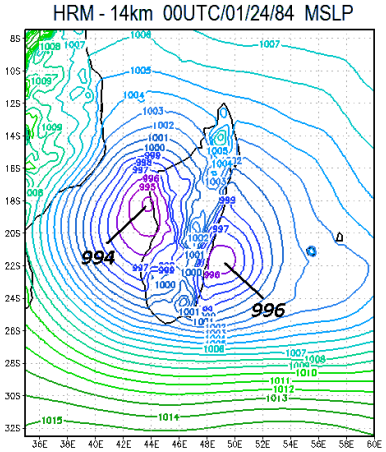

HRM - 14km 12UTC/01/21/84 Streamline 1000hPa

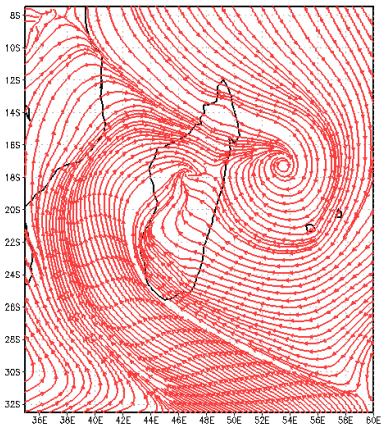

HRM - 14km 00UTC/01/22/84 Streamline 1000hPa

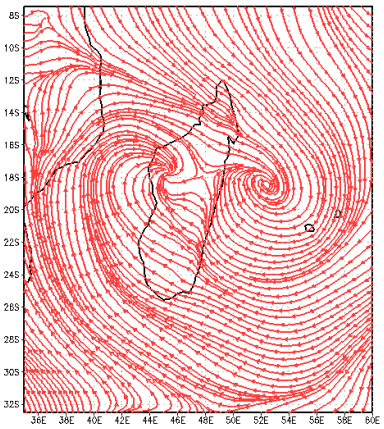

HRM - 14km 12UTC/01/22/84 Streamline 1000hPa

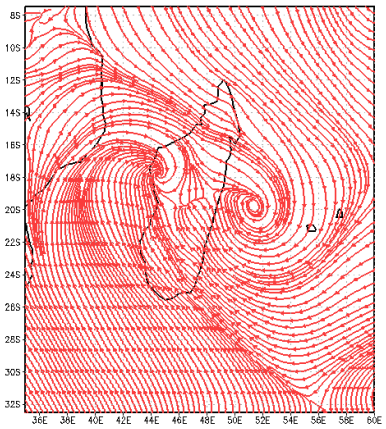

HRM - 14km 00UTC/01/23/84 Streamline 1000hPa

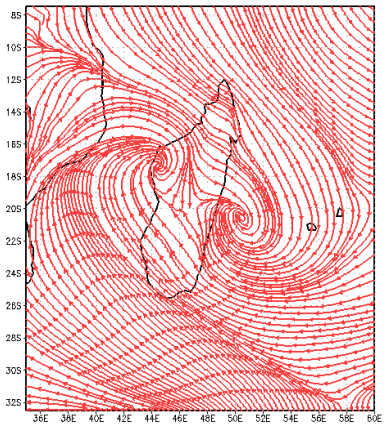

HRM - 14km 12UTC/01/23/84 Streamline 1000hPa

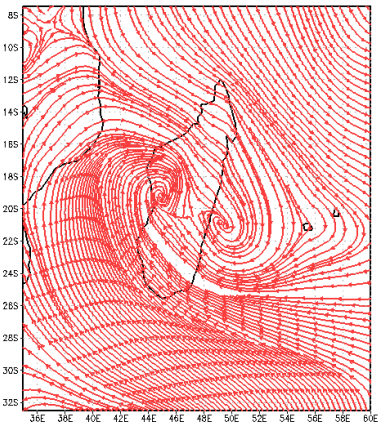

HRM - 14km 00UTC/01/24/84 Streamline 1000hPa

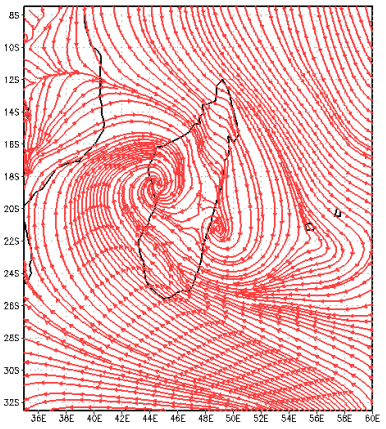

Type B1 - DOMOINA

HRM - 14km 12UTC/02/16/00 MSLP

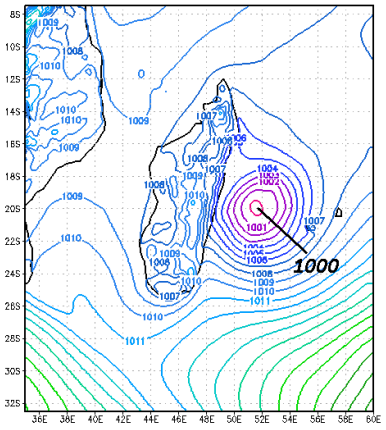

HRM - 14km 00UTC/02/17/00 MSLP

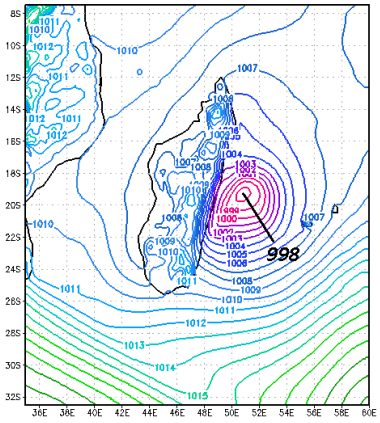

HRM - 14km 12UTC/02/17/00 MSLP

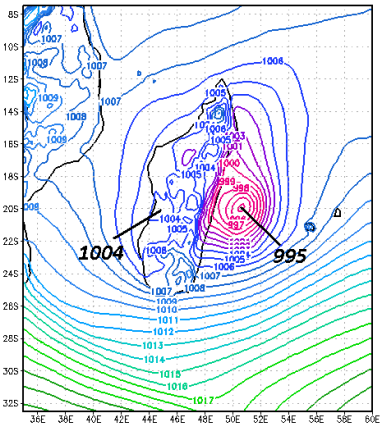

HRM - 14km 00UTC/02/18/00 MSLP

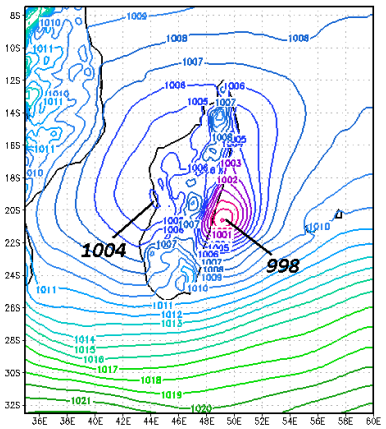

HRM - 14km 12UTC/02/18/00 MSLP

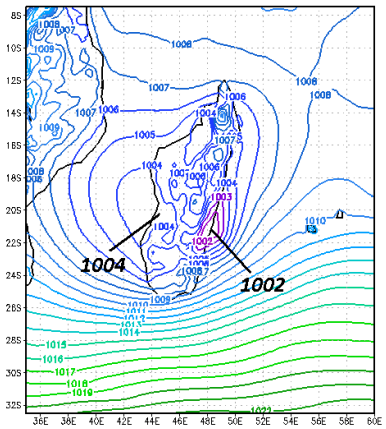

HRM - 14km 00UTC/02/19/00 MSLP

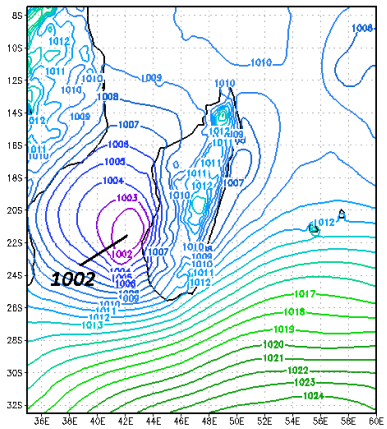

HRM - 14km 12UTC/02/16/00 Streamline 1000hPa

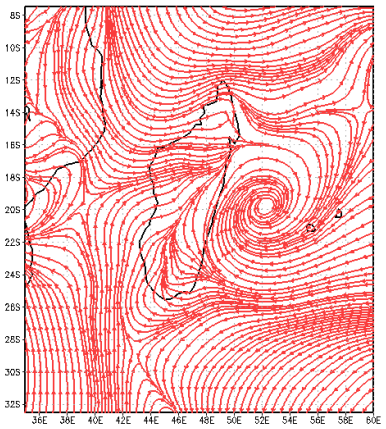

HRM - 14km 00UTC/02/17/00 Streamline 1000hPa

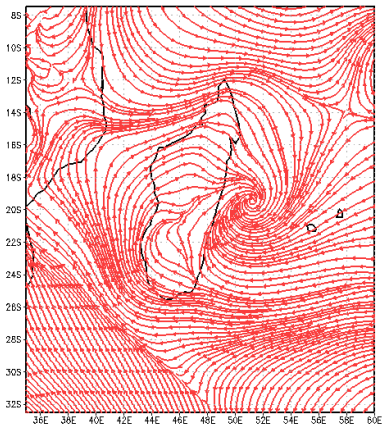

HRM - 14km 12UTC/02/17/00 Streamline 1000hPa

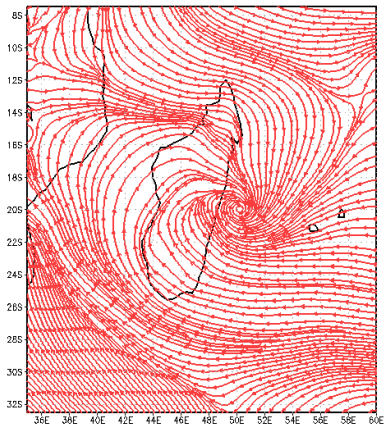

HRM - 14km 00UTC/02/18/00 Streamline 1000hPa

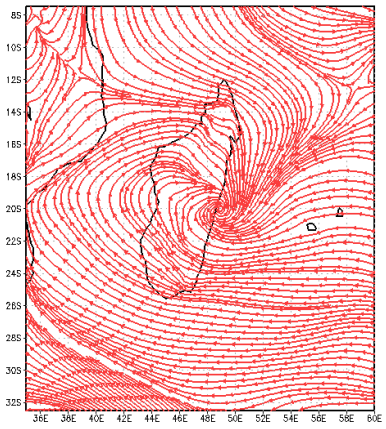

HRM - 14km 12UTC/02/18/00 Streamline 1000hPa

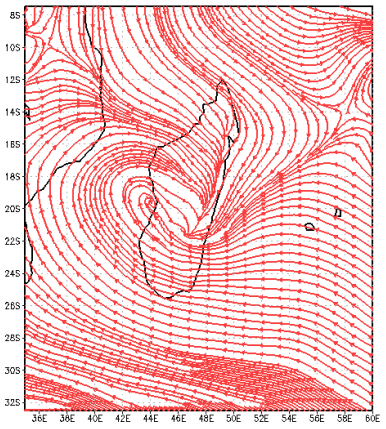

HRM - 14km 00UTC/02/19/00 Streamline 1000hPa

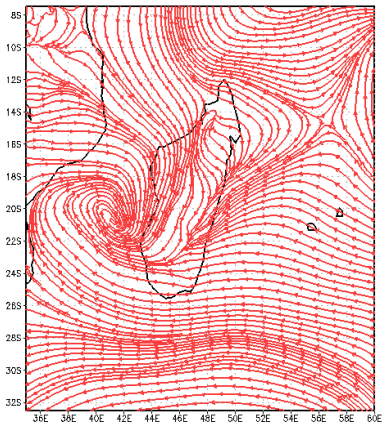

Type B1 - ELINE

Type B2 - HONORININA

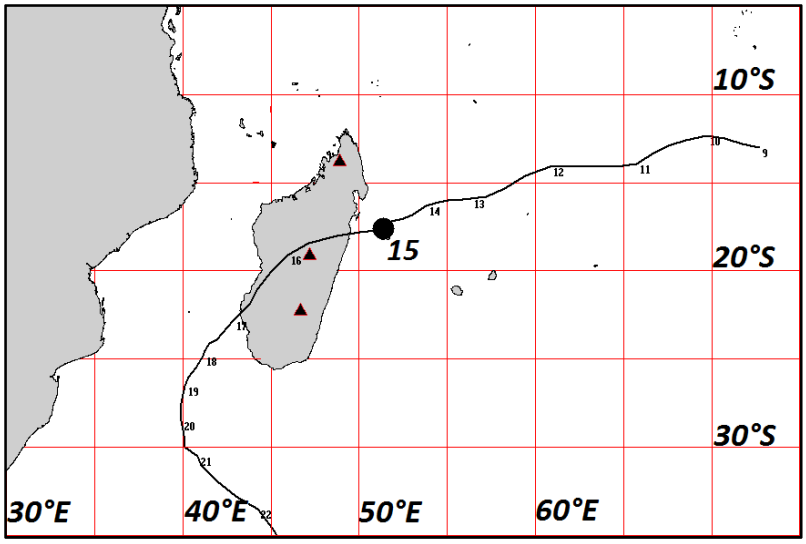

Track of cyclone HONORININA
(03/09/1986 – 03/23/1986)

Type B2 - IVAN

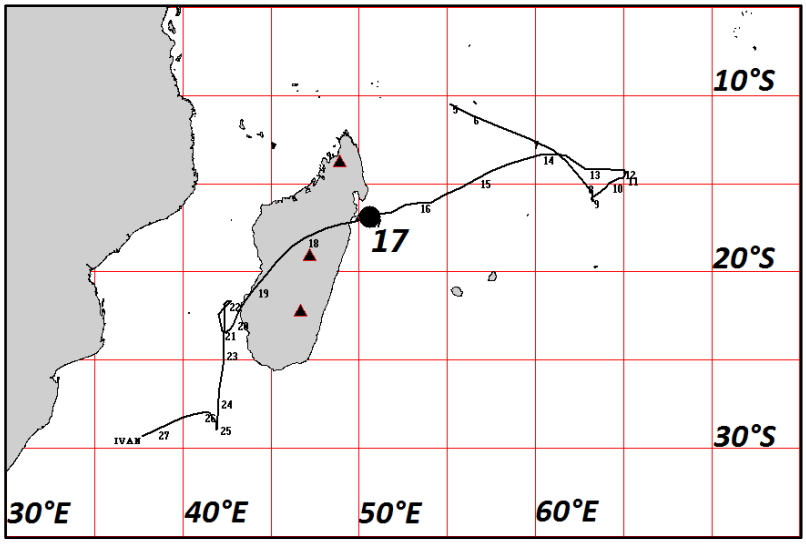

Track of cyclone IVAN
(02/05/2008 – 02/27/2008)

HRM - 14km 00UTC/03/15/86 MSLP

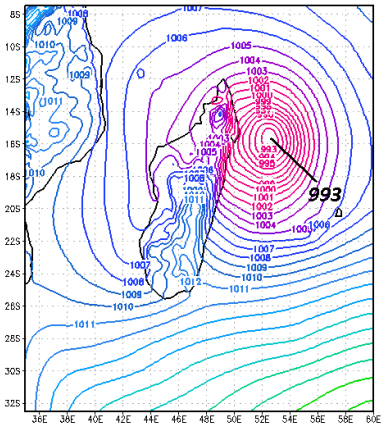

HRM - 14km 12UTC/03/15/86 MSLP

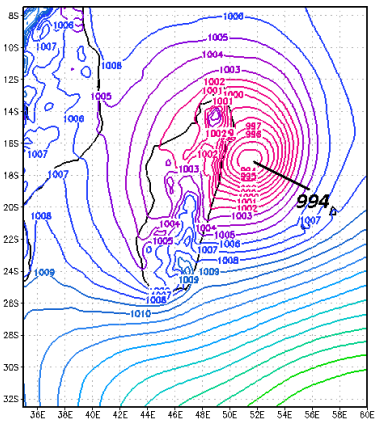

HRM - 14km 00UTC/03/16/86 MSLP

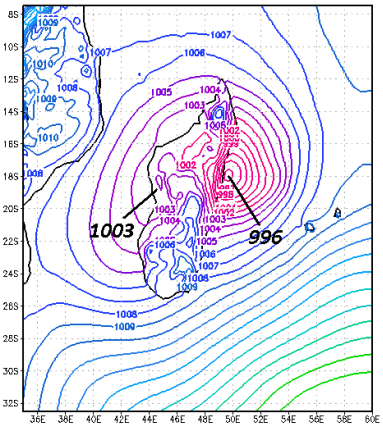

HRM - 14km 12UTC/03/16/86 MSLP

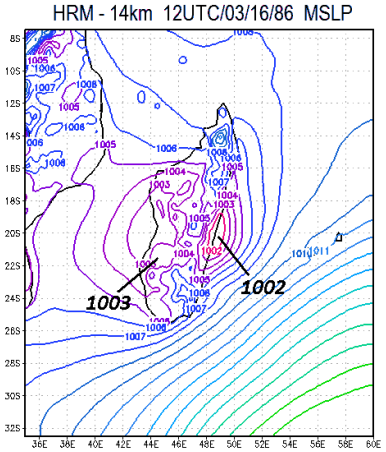

HRM - 14km 00UTC/03/17/86 MSLP

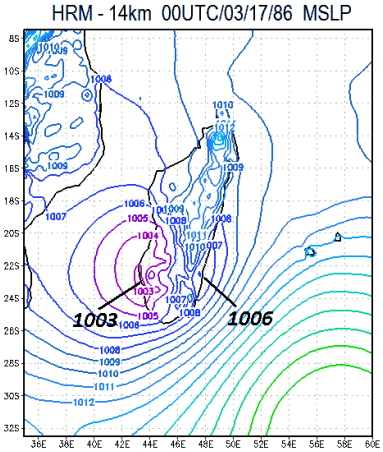

HRM - 14km 12UTC/03/17/86 MSLP

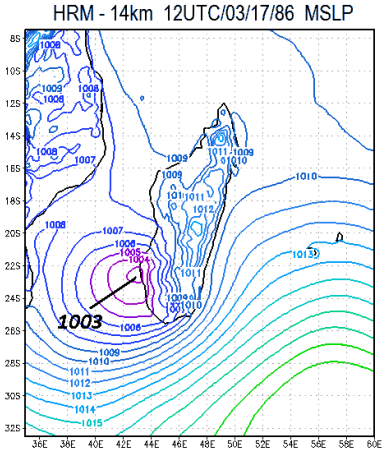

HRM - 14km 00UTC/03/15/86 Streamline 1000hPa

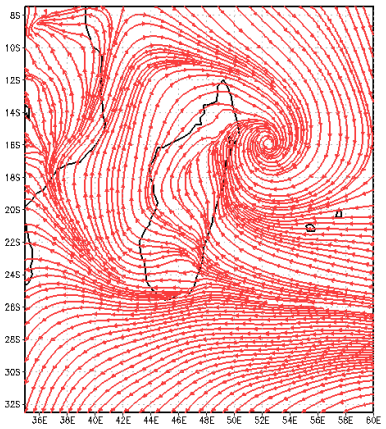

HRM - 14km 12UTC/03/15/86 Streamline 1000hPa

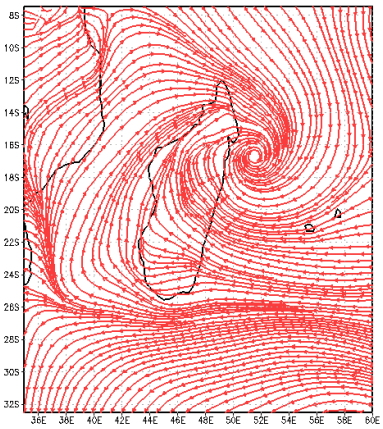

HRM - 14km 00UTC/03/16/86 Streamline 1000hPa

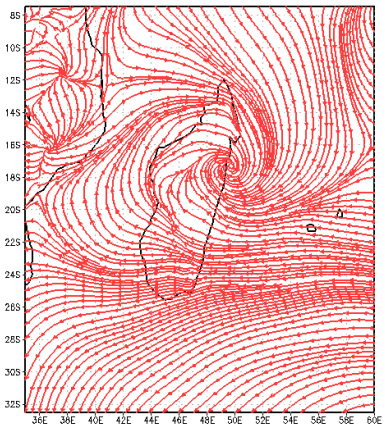

HRM - 14km 12UTC/03/16/86 Streamline 1000hPa

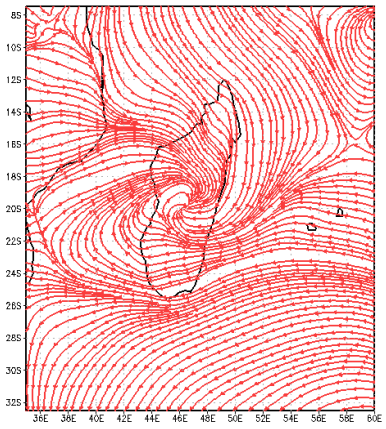

HRM - 14km 00UTC/03/17/86 Streamline 1000hPa

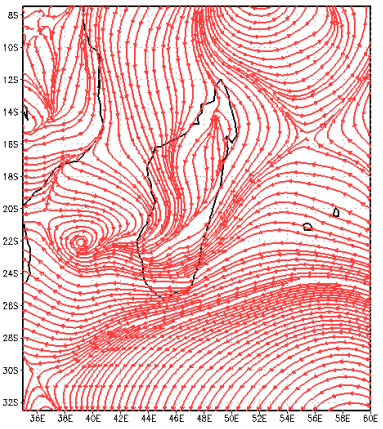

HRM - 14km 12UTC/03/17/86 Streamline 1000hPa

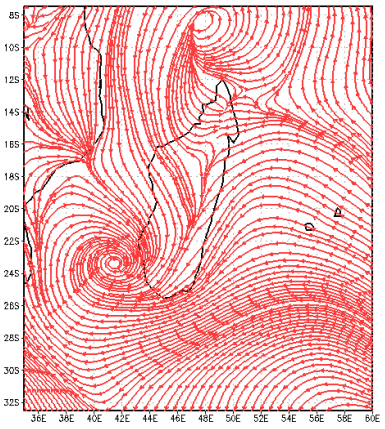

Type B2 - HONORININA

HRM - 14km 00UTC/02/16/08 MSLP

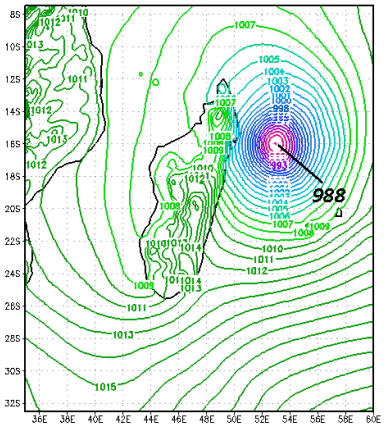

HRM - 14km 12UTC/02/16/08 MSLP

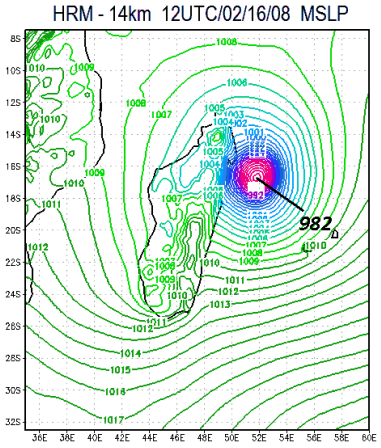

HRM - 14km 00UTC/02/17/08 MSLP

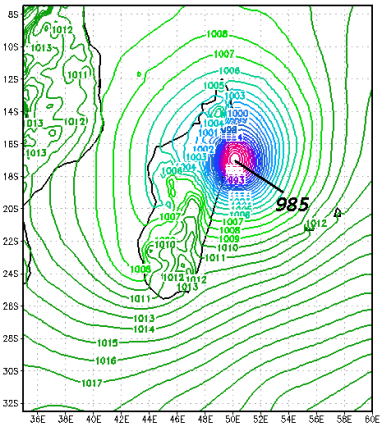

HRM - 14km 12UTC/02/17/08 MSLP

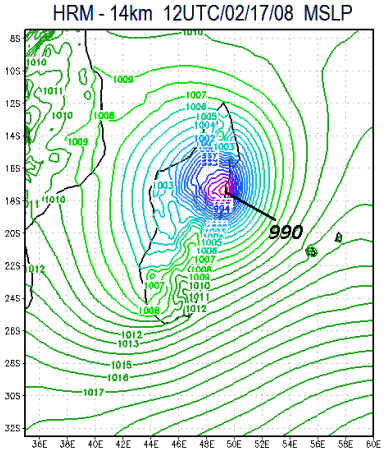

HRM - 14km 00UTC/02/18/08 MSLP

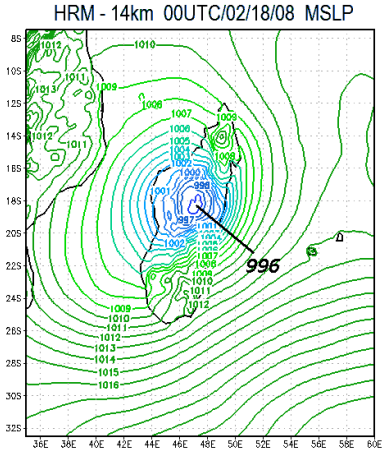

HRM - 14km 12UTC/02/18/08 MSLP

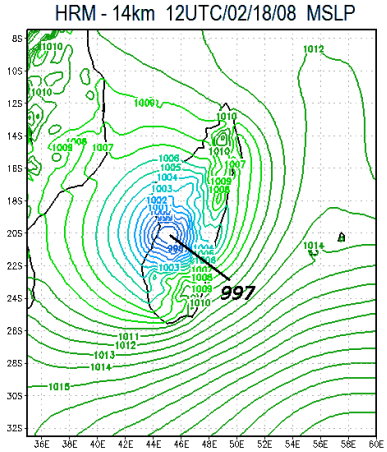

HRM - 14km 00UTC/02/16/08 Streamline 1000hPa

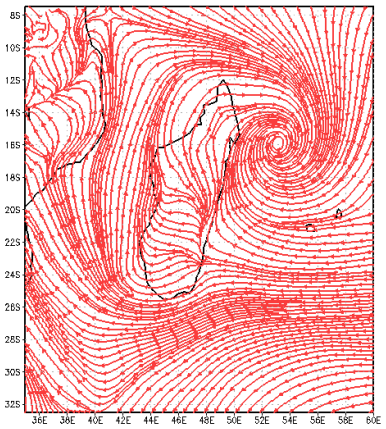

HRM - 14km 12UTC/02/16/08 Streamline 1000hPa

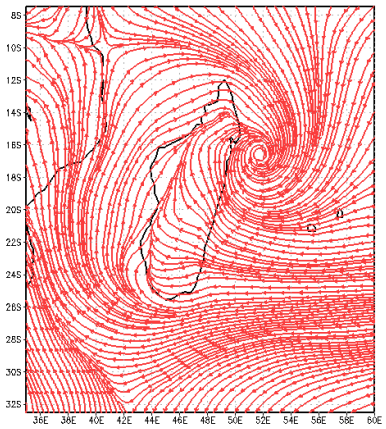

HRM - 14km 00UTC/02/17/08 Streamline 1000hPa

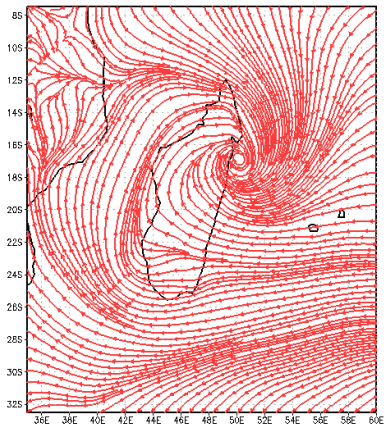

HRM - 14km 12UTC/02/17/08 Streamline 1000hPa

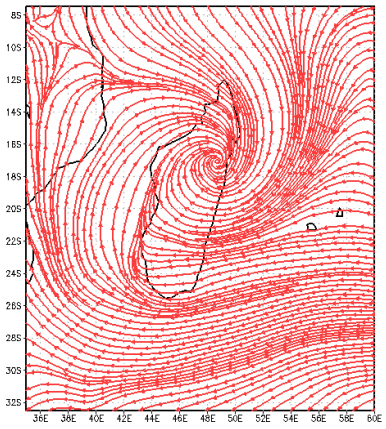

HRM - 14km 00UTC/02/18/08 Streamline 1000hPa

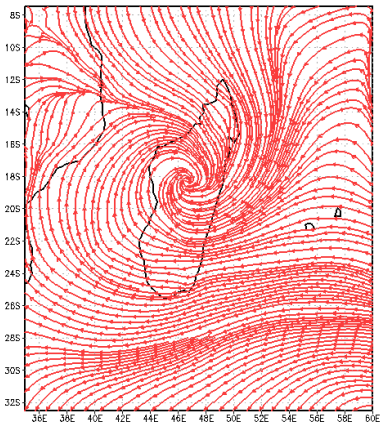

HRM - 14km 12UTC/02/18/08 Streamline 1000hPa

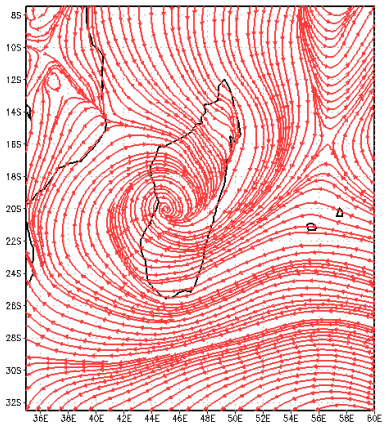

Type B2 - IVAN

Type C - FARI

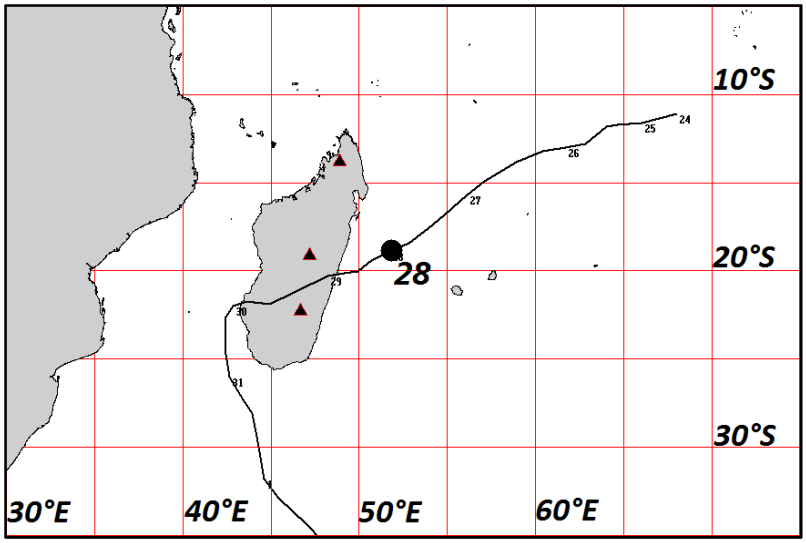

Track of cyclone FARI
(01/24/2003 – 02/02/2003)

Type C - GRETELLE

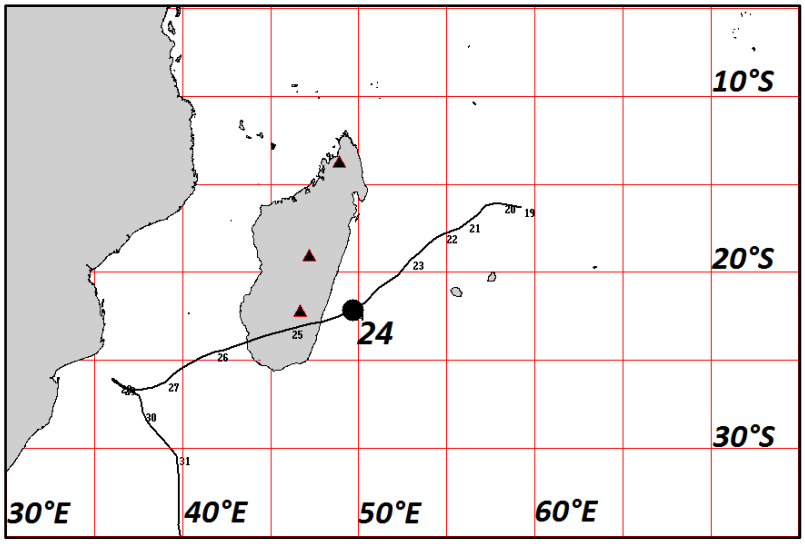

Track of cyclone GRETELLE
(01/19/1997 – 01/31/1997)

HRM - 14km 00UTC/01/27/03 MSLP

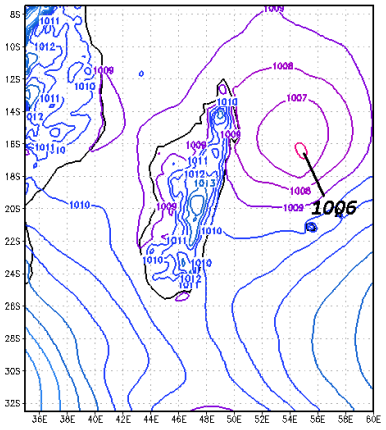

HRM - 14km 12UTC/01/27/03 MSLP

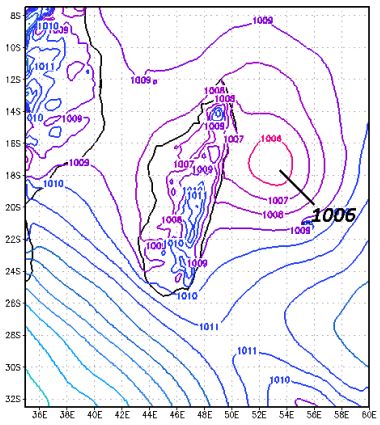

HRM - 14km 00UTC/01/28/03 MSLP

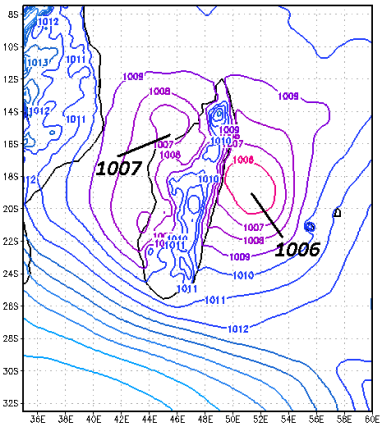

HRM - 14km 12UTC/01/28/03 MSLP

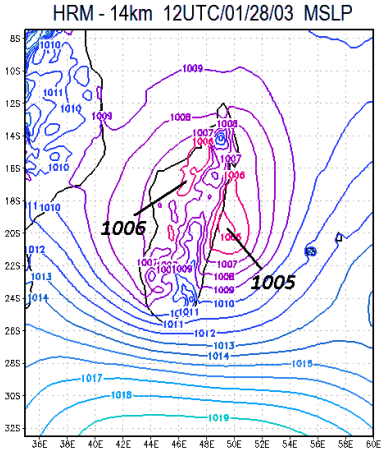

HRM - 14km 00UTC/01/29/03 MSLP

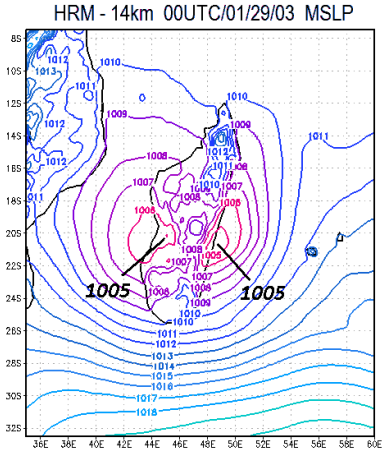

HRM - 14km 12UTC/01/29/03 MSLP

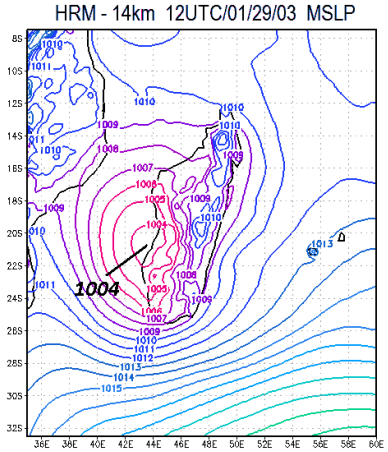

HRM - 14km 00UTC/01/27/03 Streamline 1000hPa

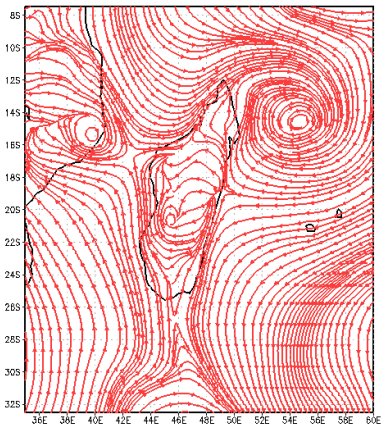

HRM - 14km 12UTC/01/27/03 Streamline 1000hPa

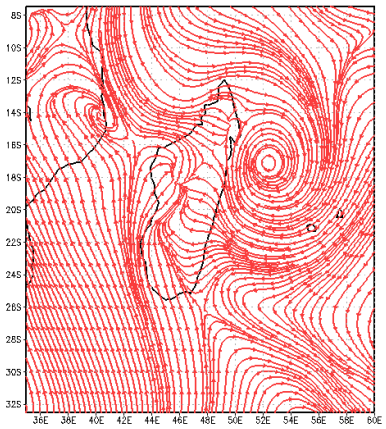

HRM - 14km 00UTC/01/28/03 Streamline 1000hPa

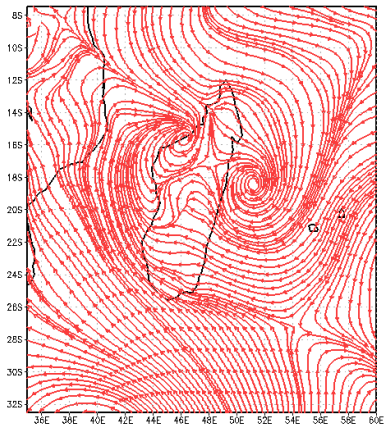

HRM - 14km 12UTC/01/28/03 Streamline 1000hPa

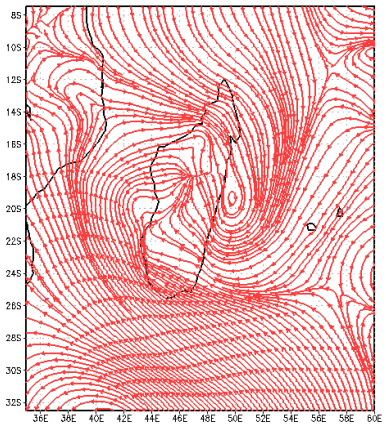

HRM - 14km 00UTC/01/29/03 Streamline 1000hPa

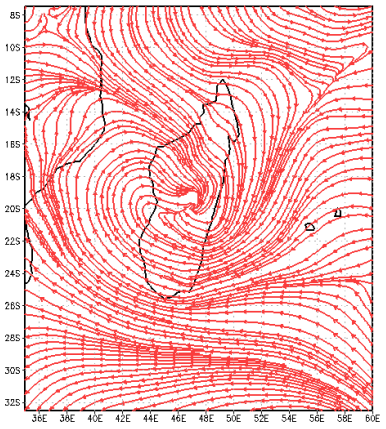

HRM - 14km 12UTC/01/29/03 Streamline 1000hPa

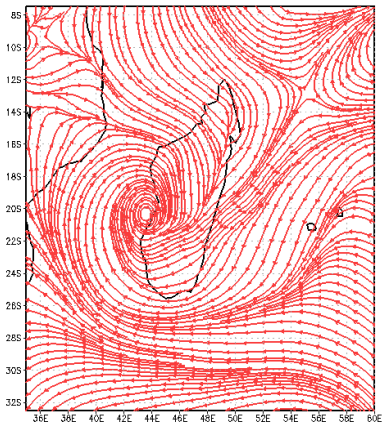

Type C - FARI

HRM - 14km 00UTC/01/23/97 MSLP

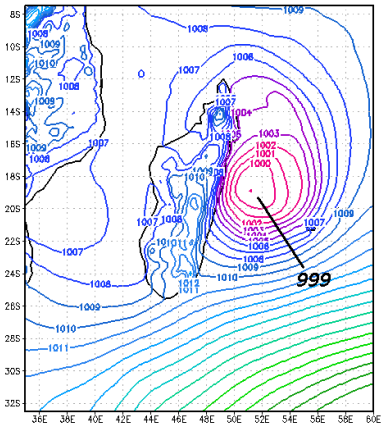

HRM - 14km 12UTC/01/23/97 MSLP

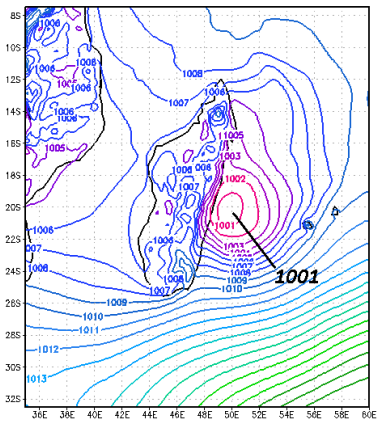

HRM - 14km 00UTC/01/24/97 MSLP

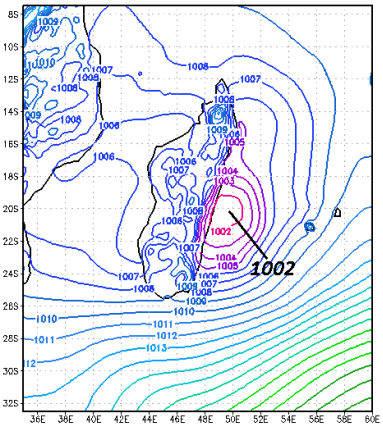

HRM - 14km 12UTC/01/24/97 MSLP

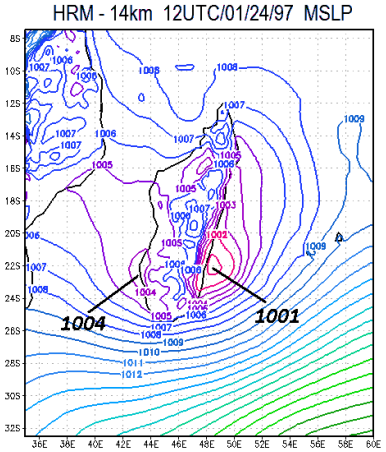

HRM - 14km 00UTC/01/25/97 MSLP

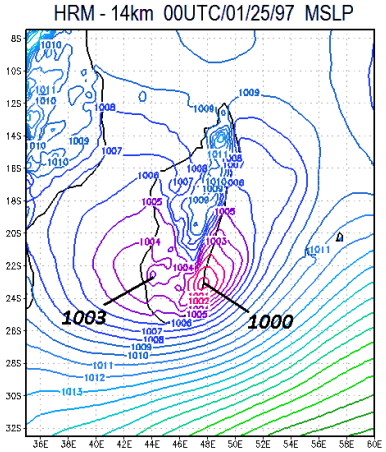

HRM - 14km 12UTC/01/25/97 MSLP

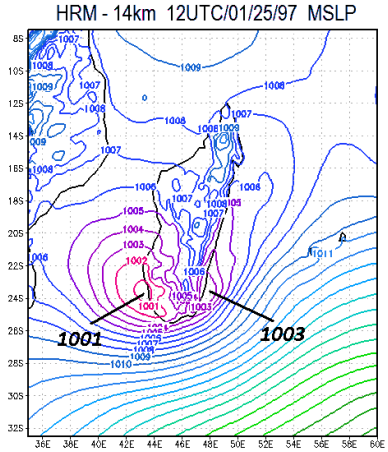

HRM - 14km 00UTC/01/23/97 Streamline 1000hPa

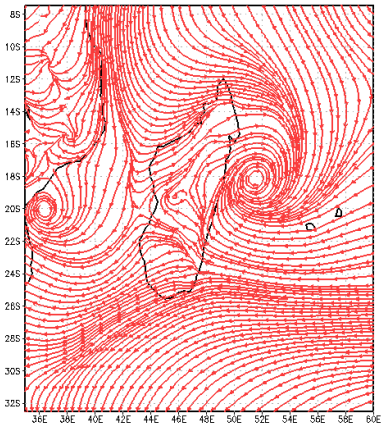

HRM - 14km 12UTC/01/23/97 Streamline 1000hPa

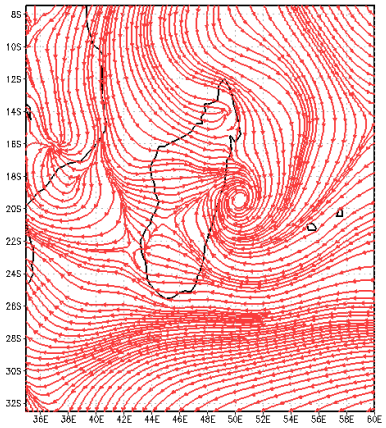

HRM - 14km 00UTC/01/24/97 Streamline 1000hPa

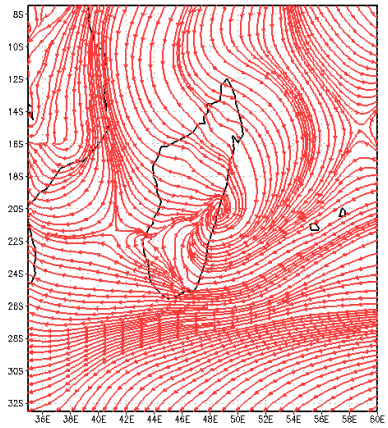

HRM - 14km 12UTC/01/24/97 Streamline 1000hPa

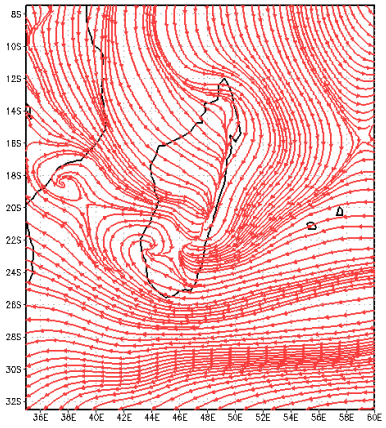

HRM - 14km 00UTC/01/25/97 Streamline 1000hPa

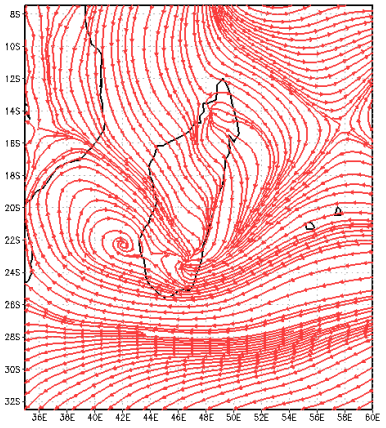

HRM - 14km 12UTC/01/25/97 Streamline 1000hPa

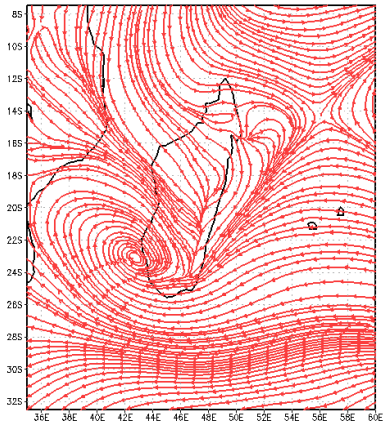

Type C - GRETELLE

Type D - LITANNE

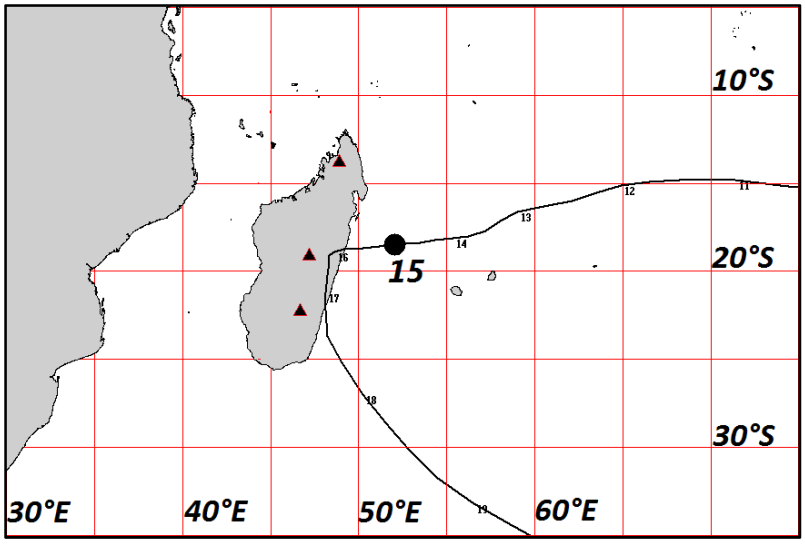

Track of cyclone LITANNE
(03/07/1994 – 03/19/1994)

Type D - JADE

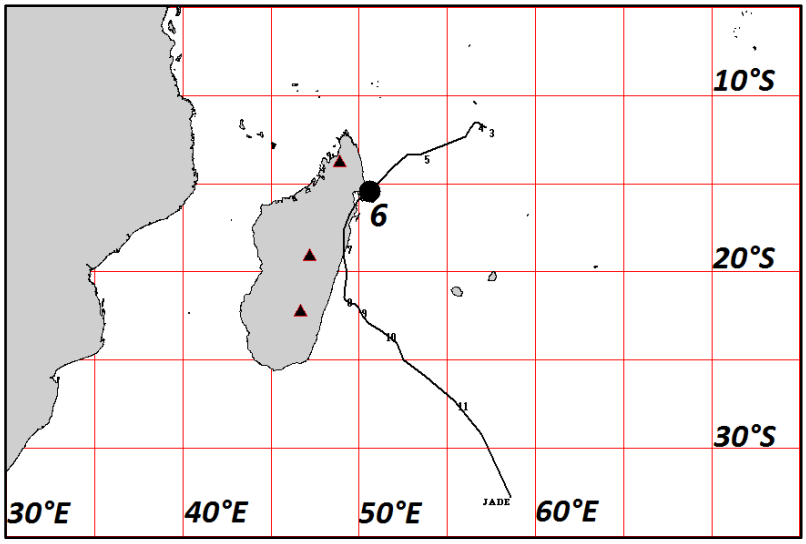

Track of cyclone JADE
(04/03/2009 – 04/11/2009)

HRM - 14km 00UTC/03/15/94 MSLP

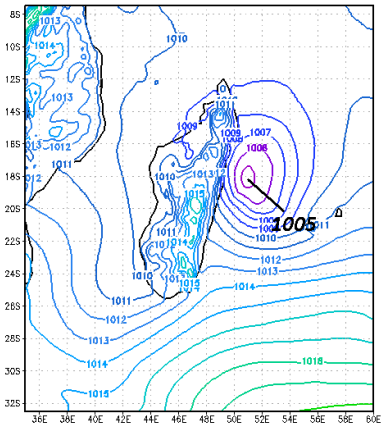

HRM - 14km 12UTC/03/15/94 MSLP

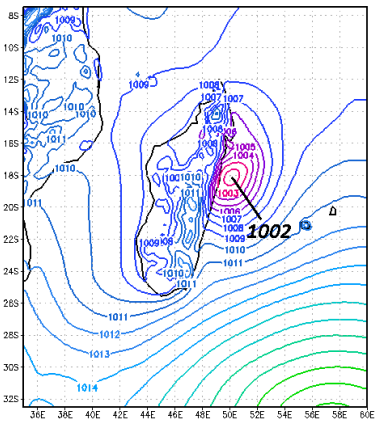

HRM - 14km 00UTC/03/16/94 MSLP

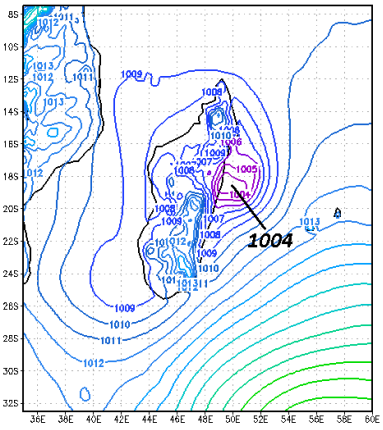

HRM - 14km 12UTC/03/16/94 MSLP

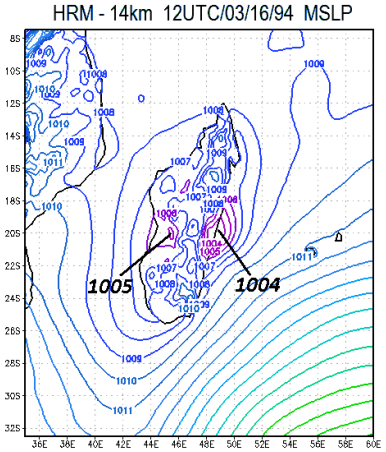

HRM - 14km 00UTC/03/17/94 MSLP

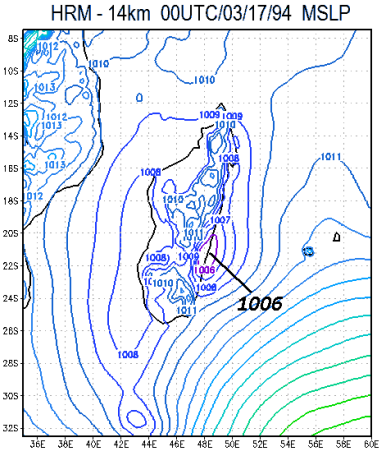

HRM - 14km 12UTC/03/17/94 MSLP

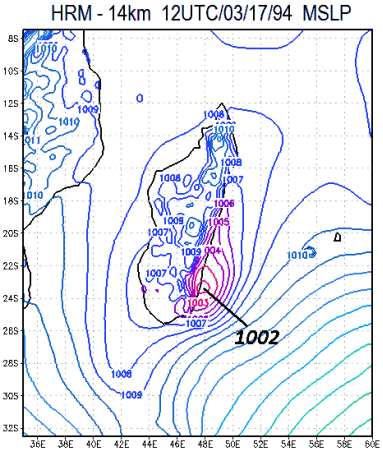

HRM - 14km 00UTC/03/15/94 Streamline 1000hPa

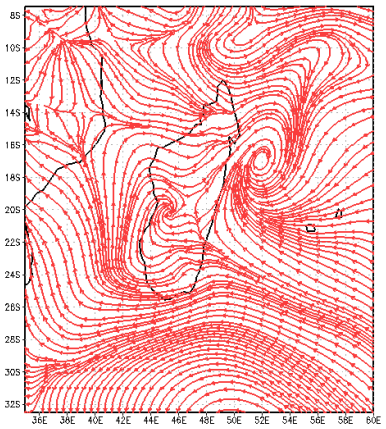

HRM - 14km 12UTC/03/15/94 Streamline 1000hPa

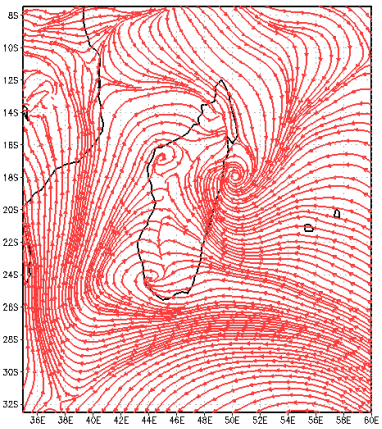

HRM - 14km 00UTC/03/16/94 Streamline 1000hPa

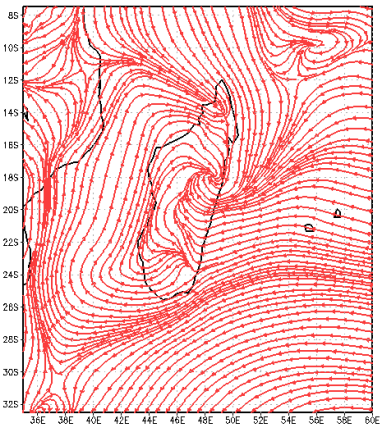

HRM - 14km 12UTC/03/16/94 Streamline 1000hPa

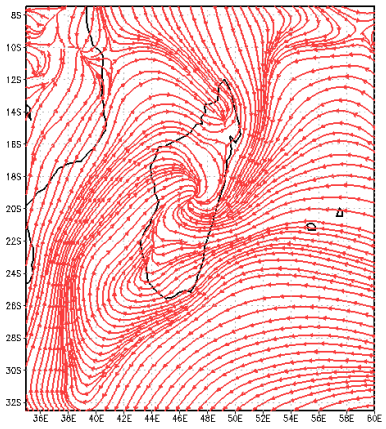

HRM - 14km 00UTC/03/17/94 Streamline 1000hPa

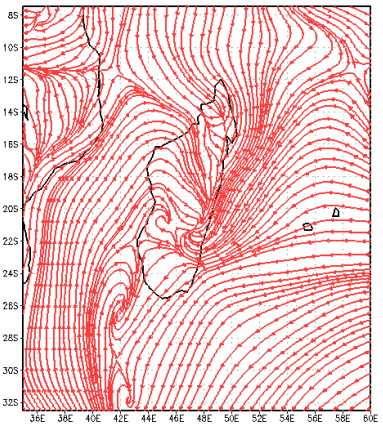

HRM - 14km 12UTC/03/17/94 Streamline 1000hPa

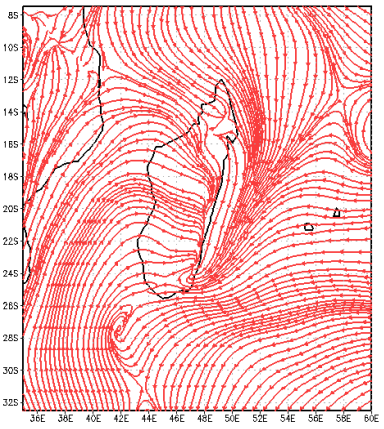

Type D - LITANNE

HRM - 14km 00UTC/04/06/09 MSLP

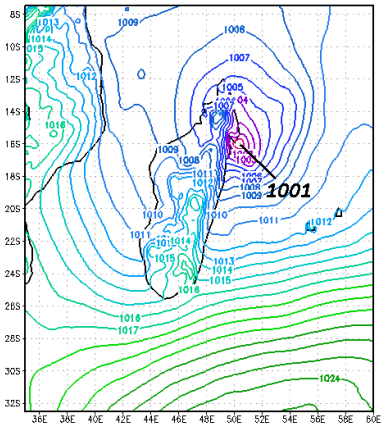

HRM - 14km 12UTC/04/06/09 MSLP

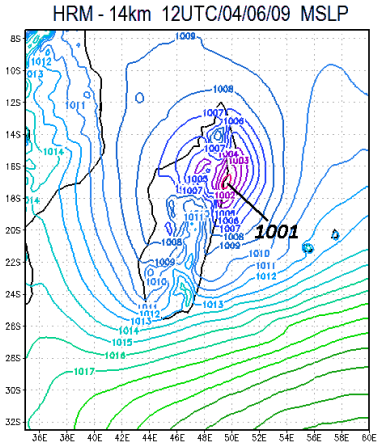

HRM - 14km 00UTC/04/07/09 MSLP

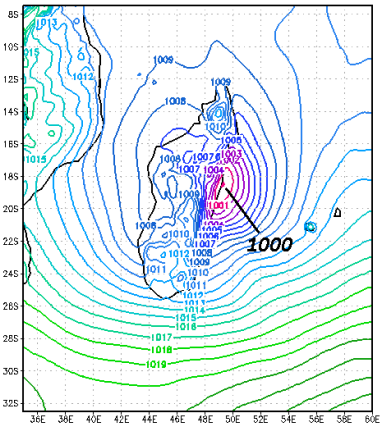

HRM - 14km 12UTC/04/07/09 MSLP

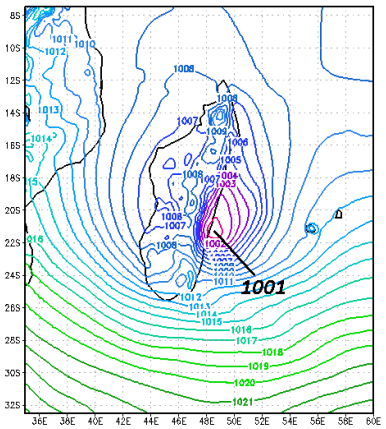

HRM - 14km 00UTC/04/08/09 MSLP

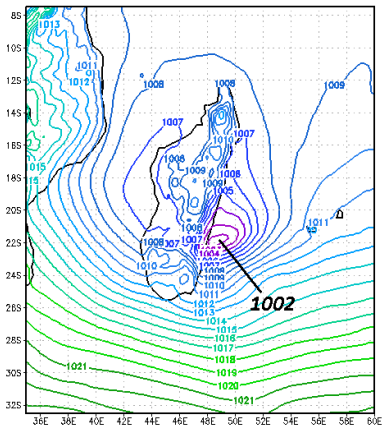

HRM - 14km 12UTC/04/08/09 MSLP

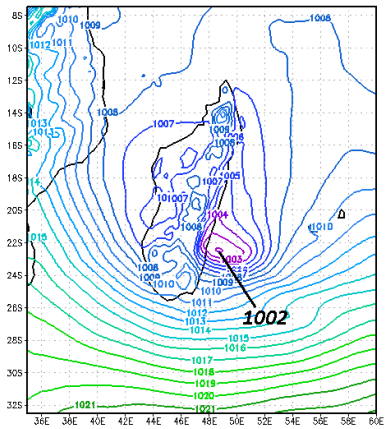

HRM - 14km 00UTC/04/06/09 Streamline 1000hPa

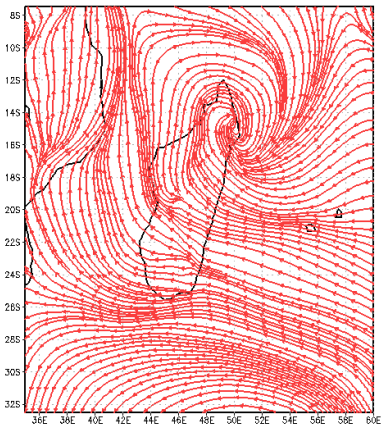

HRM - 14km 12UTC/04/06/09 Streamline 1000hPa

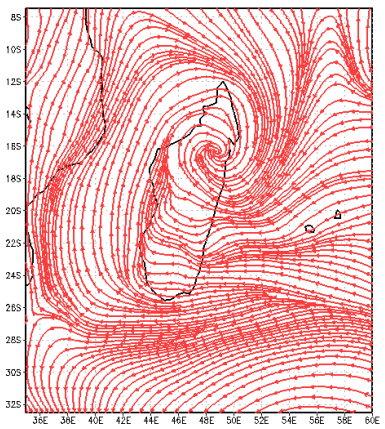

HRM - 14km 00UTC/04/07/09 Streamline 1000hPa

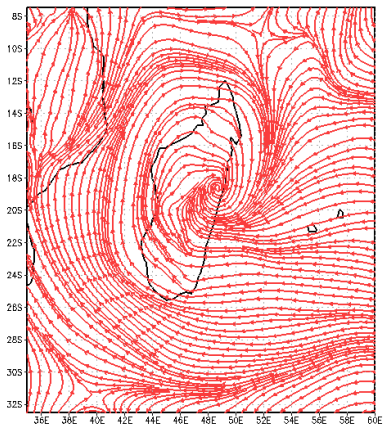

HRM - 14km 12UTC/04/07/09 Streamline 1000hPa

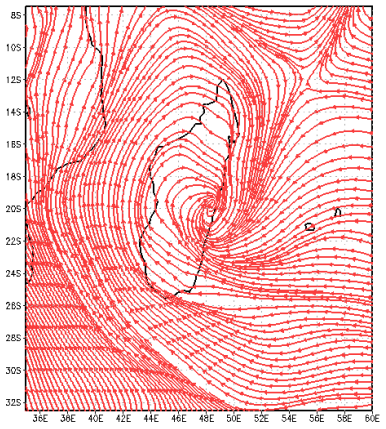

HRM - 14km 00UTC/04/08/09 Streamline 1000hPa

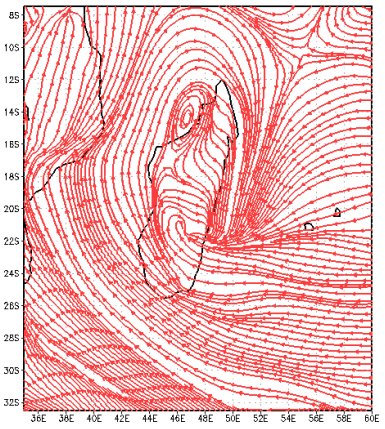

HRM - 14km 12UTC/04/08/09 Streamline 1000hPa

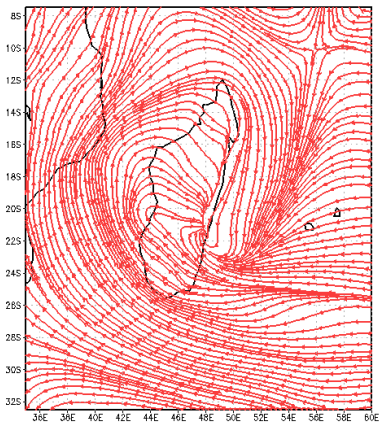

Type D - JADE

Type E - HELY

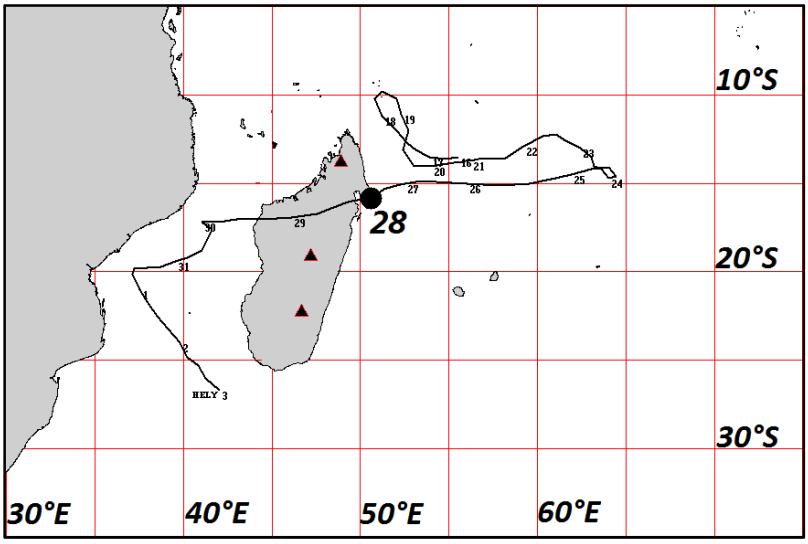

Track of cyclone HELY
(03/16/1988 – 04/03/1988)

Type E - ALIBERA

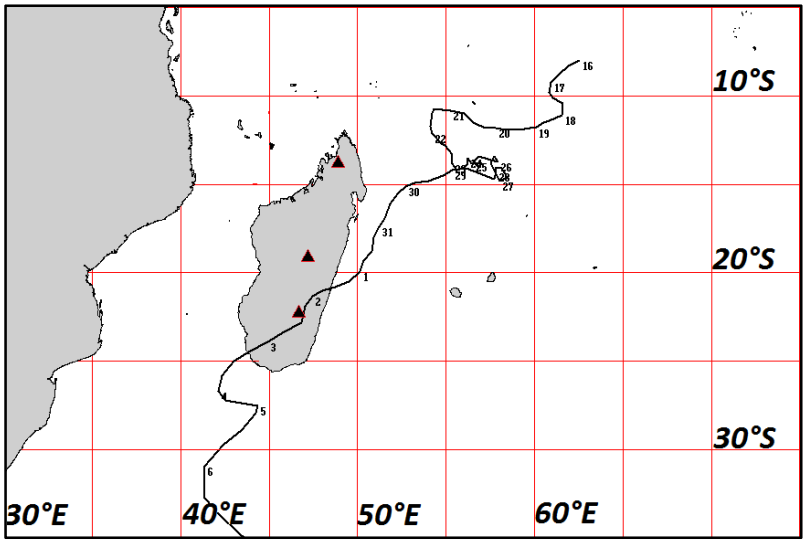

Track of cyclone ALIBERA
(12/16/1990 – 01/07/1990)

HRM - 14km 00UTC/03/27/88 MSLP

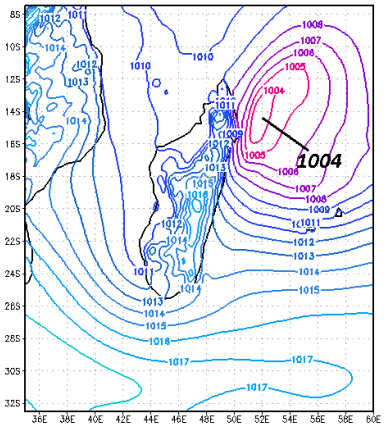

HRM - 14km 12UTC/03/27/88 MSLP

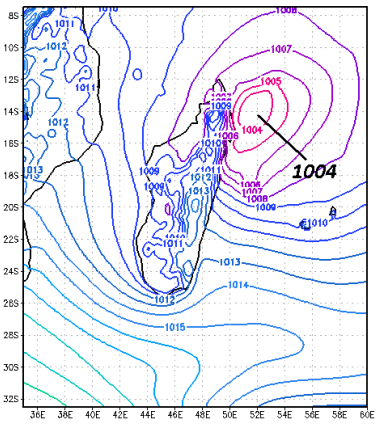

HRM - 14km 00UTC/03/28/88 MSLP

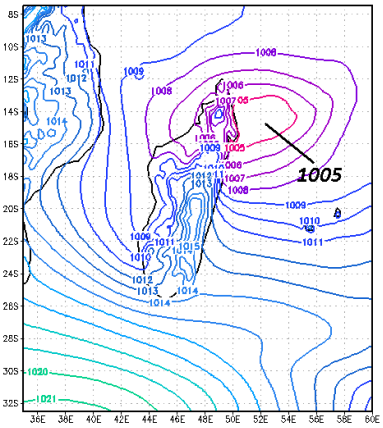

HRM - 14km 12UTC/03/28/88 MSLP

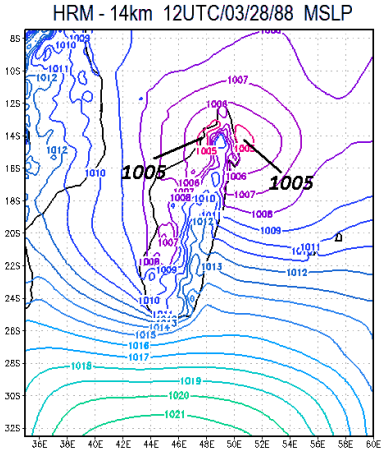

HRM - 14km 00UTC/03/29/88 MSLP

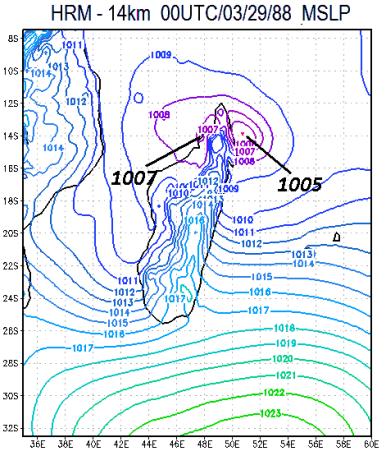

HRM - 14km 12UTC/03/29/88 MSLP

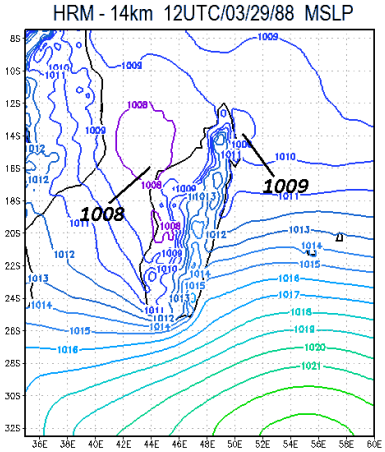

HRM - 14km 00UTC/03/27/88 Streamline 1000hPa

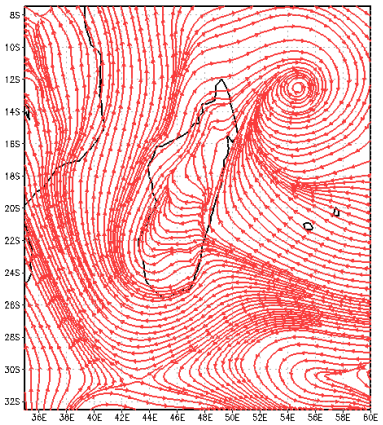

HRM - 14km 12UTC/03/27/88 Streamline 1000hPa

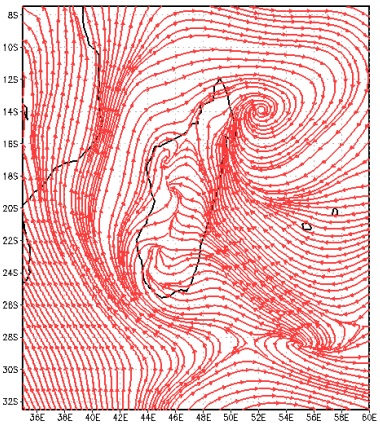

HRM - 14km 00UTC/03/28/88 Streamline 1000hPa

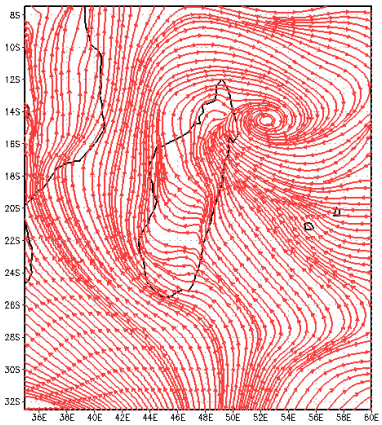

HRM - 14km 12UTC/03/28/88 Streamline 1000hPa

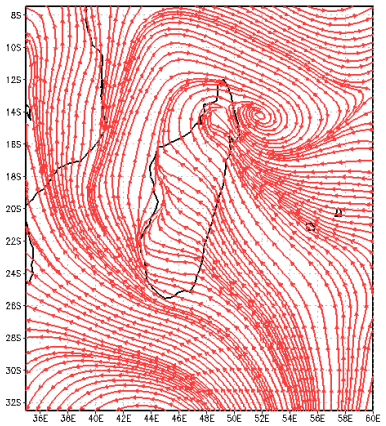

HRM - 14km 00UTC/03/29/88 Streamline 1000hPa

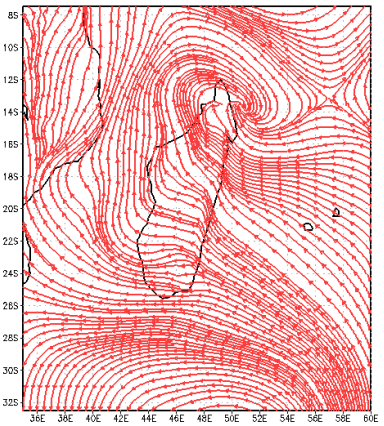

HRM - 14km 12UTC/03/29/88 Streamline 1000hPa

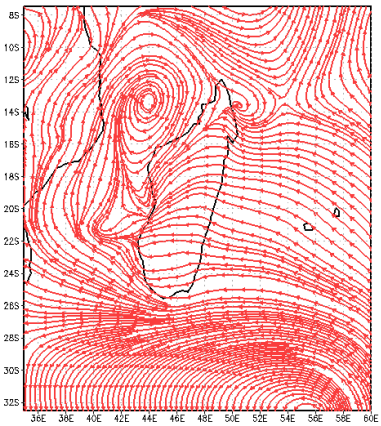

Type E - HELY

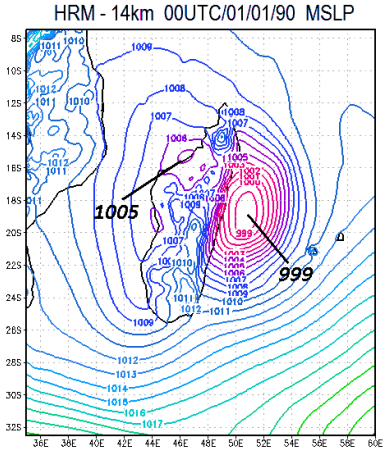

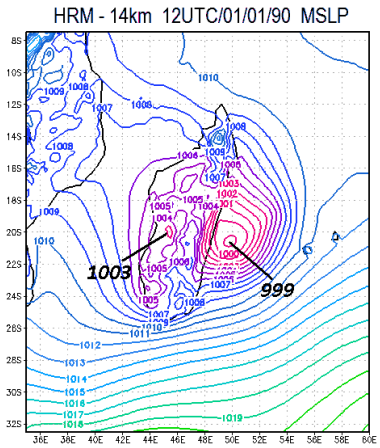

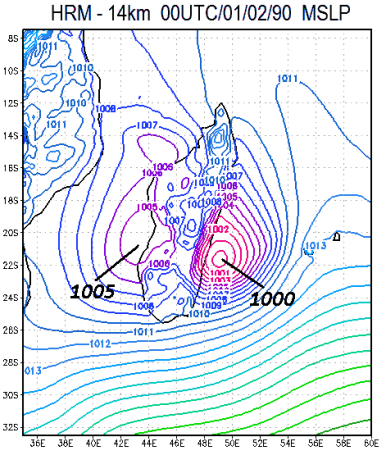

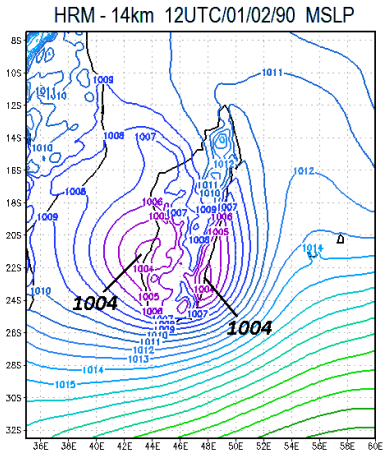

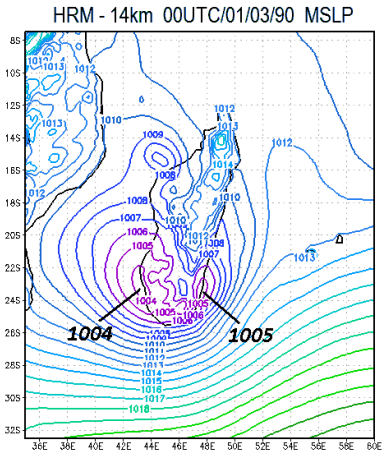

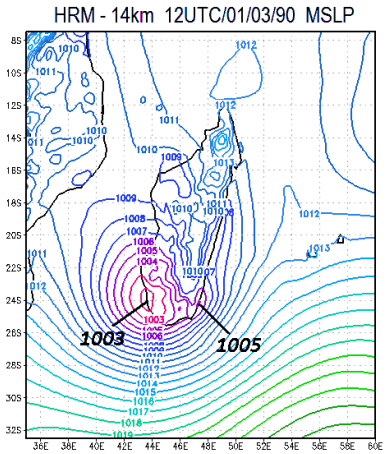

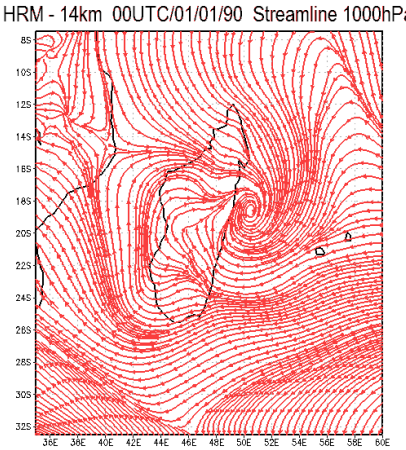

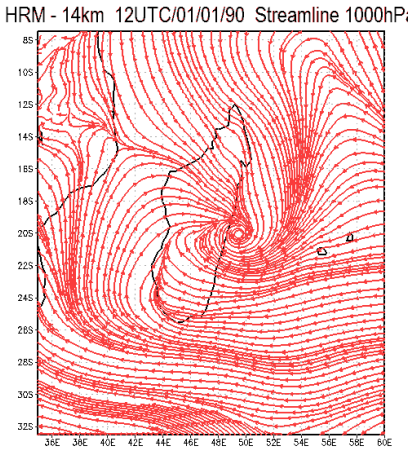

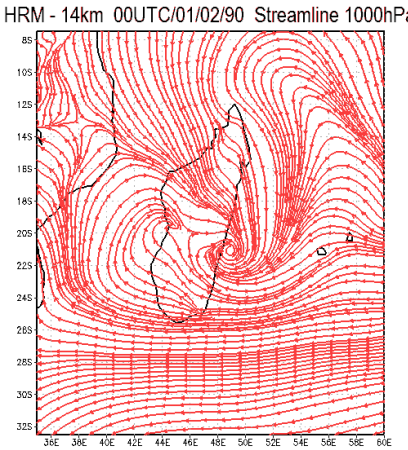

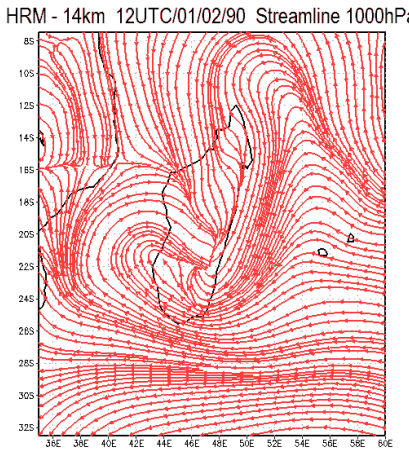

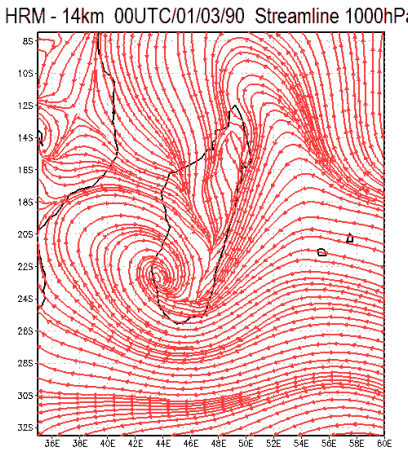

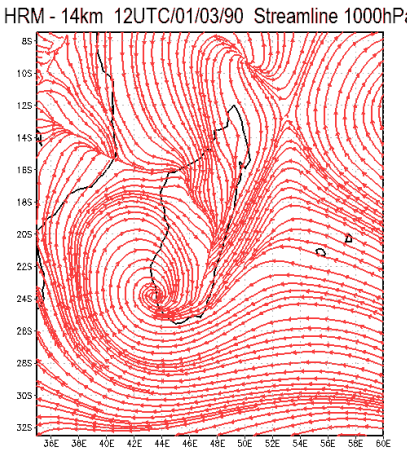

Type E - ALIBERA